Fabrication and Printing of Multi-material Hydrogels

Navein Arumugasaamy, Hannah B. Baker, David S. Kaplan, Peter C. W. Kim, and John P. Fisher

Contents

1 Introduction 398
2 Challenges Associated with Hydrogel Bioprinting 399
2.1 Choice of Bioprinter 400
2.2 Mechanical Support and Printability 402
2.3 Stress in Cell-Laden Hydrogels 404
3 Methods for Polymer Crosslinking 405
3.1 Photo-crosslinking 405

N. Arumugasaamy · J. P. Fisher (✉)
Fischell Department of Bioengineering, University of Maryland, College Park, MD, USA

Sheikh Zayed Institute for Pediatric Surgical Innovation, Children's National Health System, Washington, DC, USA
e-mail: navein@umd.edu; jpfisher@umd.edu

H. B. Baker
Fischell Department of Bioengineering, University of Maryland, College Park, MD, USA

Center for Devices and Radiological Health, U.S. Food and Drug Administration, Silver Spring, MD, USA
e-mail: hbaker1@umd.edu

D. S. Kaplan
Center for Devices and Radiological Health, U.S. Food and Drug Administration, Silver Spring, MD, USA
e-mail: David.Kaplan@fda.hhs.gov

P. C. W. Kim
Sheikh Zayed Institute for Pediatric Surgical Innovation, Children's National Health System, Washington, DC, USA

School of Medicine and Health Sciences, The George Washington University, Washington, DC, USA
e-mail: PKim@childrensnational.org

© This is a U.S. Government work and not under copyright protection in the US; foreign copyright protection may apply 2018

A. Ovsianikov et al. (eds.), *3D Printing and Biofabrication*, Reference Series in Biomedical Engineering, https://doi.org/10.1007/978-3-319-45444-3_13

3.2 Thermal Crosslinking 408
3.3 Ionic Crosslinking 408
4 Multi-material Hydrogel Printing 409
4.1 Material Selection 409
4.2 Common Materials in Hydrogel Bioprinting 411
4.3 Single Bioink Bioprinting 414
4.4 Multiple Bioink Bioprinting 420
5 Summary and Future Directions 422
References 423

Abstract

Bioprinting has emerged over the past decade as a prominent technology in the field of tissue engineering. This enables fabrication of cell-laden hydrogels with precise control over the architecture of the scaffold and the location of cells, growth factors, and other biological cues of interest. We first discuss the challenges that exist in terms of choosing a bioprinter, ensuring mechanical support and printability of a material, and minimizing cellular stress for cell-laden prints. We then explain the different crosslinking methods commonly used in hydrogel printing and approaches to alter bioink crosslinking mechanisms. We discuss material selection for bioprinting with elaboration on common materials that have been used and a review of multi-material prints involving hydrogels. We also explore the use of a single, mixed bioink to fabricate complex but homogeneous constructs and multiple, independent bioinks to fabricate complex heterogeneous tissue constructs within the multi-material review. We conclude with a summary of the current state of the field and an outlook on future research.

1 Introduction

Hydrogels are networks of crosslinked, hydrophilic polymers capable of absorbing water and swelling in size. They have long been used in a variety of applications, such as for drug delivery, where their ability to swell and degrade can be utilized to deliver molecules of various sizes and chemical structure, and in tissue engineering, where hydrogels provide a support environment for encapsulating and growing cells in a 3D biomimetic environment (Qiu and Park 2001; Hoare and Kohane 2008; Burdick and Prestwich 2011; Murphy and Atala 2014; Pereira and Bártolo 2015). In particular, hydrogels have become prominent in applications involving cells, due to the capacity to mimic the native in vivo cellular environment. For this reason, hydrogels have become common as an alternative to traditional solid material scaffolds for cell growth and assays in a 3D environment. In applications using solid scaffolds, cells are grown on the surface of the material wherein the bulk material properties, such as porosity and pore size, influence cell growth and behavior. With hydrogels, cells can be fully encapsulated in the material, providing cells with a means to directly interact with their scaffold in three dimensions. This differs from traditional scaffolds, in which cells interact with the scaffold via cell-scaffold

adhesion points on the surface. Further, it is worth noting that many groups have investigated the use of cell suspensions alone as bioinks to generate patterns and to spatially arrange multiple cell types on one substrate (Roth et al. 2004; Nakamura et al. 2005; Xu et al. 2013b, 2005, 2006; Carolina 2012; Ferris et al. 2013a, b; Skardal and Atala 2015). However, these approaches when used without a supporting matrix are better suited for sheet-like applications, such as drug delivery, and cannot offer the same therapeutic capacity enabled by support materials (Chan et al. 2010; Cha et al. 2014; Akkineni et al. 2015; Elomaa et al. 2015; Park et al. 2015; Gao et al. 2015b; Tabriz et al. 2015; Ferlin et al. 2016). Thus, it becomes clear that hydrogels may provide an enhanced biomimetic microenvironment through improved cell-scaffold interfaces.

Fabricating hydrogels has commonly been done through the use of molds and casting, but the emergence of 3D printing (3DP) technology has allowed for significantly more spatial control of the architecture and design of the hydrogel network. Fabricating hydrogels in a mold involves filling a predefined bulk architecture with the material being used to synthesize the hydrogel, followed by crosslinking of the hydrogel within the mold such that the material transitions from liquid to solid and maintains that bulk geometry. 3DP overcomes this key limitation by depositing and crosslinking material, layer by layer, in order to control both the micro- and macro-architecture of the gel. This allows for precision, defined by the resolution of the individual bioprinter, which can go down to the microscale. Furthermore, bioprinting incorporates cells and other biological components in order to create a system for studying biological phenomena or for tissue regeneration. As a result, bioprinting enables precise control over where cells or other factors are located within the gel, as well as allowing for the use of multiple, distinct bioinks composed of unique materials or cells.

With that in mind, this chapter seeks to provide an overview of cell-laden printing of hydrogels. In particular, we discuss the current challenges in hydrogel printing and the key aspects of cell bioprinting. We provide an overview of materials commonly used, show examples of what has been done using multiple materials with different 3DP systems, and finish with commentary about what is in store for the future of hydrogel bioprinting.

2 Challenges Associated with Hydrogel Bioprinting

Although hydrogels provide a biomimetic environment for cells similar to that found in vivo, challenges remain in printing hydrogels with highly controlled architecture, maintaining mechanical support, crosslinking the polymer network while maintaining cell viability, and minimizing cellular exposure to stress. While 3DP provides precise and accurate control over the architecture, the level of precision and accuracy are largely determined by the printer used. Further, to maintain the desired level of precision and accuracy, structural support is necessary throughout the duration of the printing process. This mechanical support comes from the viscosity of the gelatinous material in the cartridge during the printing process and through the use of crosslinking,

either layer by layer or on the bulk geometry, during the printing process. Finally, the mechanism of crosslinking and the imparted shear stress need to be considered when printing cells in order to reduce cytotoxicity and mechanical damage to the cells.

2.1 Choice of Bioprinter

Currently, there are four common types of bioprinters used for 3DP hydrogels. These are inkjet bioprinters, laser-assisted bioprinters, extrusion (or micro-extrusion) bioprinters, and stereolithography (SLA) printers. Each type has been thoroughly described in recent reviews (Murphy and Atala 2014; Pereira and Bártolo 2015); thus, our emphasis here is the advantages and disadvantages of each type in printing cell-laden hydrogels. The four printing methods are depicted in Fig. 1.

Inkjet bioprinters function by dispensing small droplets of bioink onto a platform. Early inkjet printers were commercially available printers, such as Hewlett-Packard printers, modified in order to control the z-axis (Xu et al. 2005). Ink cartridges are replaced with bioink, and all parts of the printer are sterilized prior to printing (Xu et al. 2013b). As with traditional inkjet printing, small volumes (picoliters) of liquid are dispensed onto a substrate. In addition, cell viability has been shown to generally be high (>90%) (Xu et al. 2013b, 2005). Thus, this platform is benefitted by a low capital cost, comparatively fast printing speed, ease of modification for printing biological components, and demonstrated high cell viability. However, droplets are forced out using high temperatures or an applied voltage, which may lead to stresses up to 20 kPa being induced on the cells (He et al. 2014). Cells may be capable of surviving stress up to 2 MPa, but the mechanical deformation resulting from stresses this high decreases cell viability significantly (down to less than 5%), indicating care should be taken to avoid mechanical damage to cells during the printing process (Ringeisen et al. 2004; Wang et al. 2008). In addition, due to the size of the droplets and the force needed to allow for printing to occur, both cell density (on the order of 1,000,000 cells/mL) and viscosity of bioink is limited (Xu et al. 2005).

Laser-assisted bioprinters operate based upon laser-induced forward transfer (Koch et al. 2012). In essence, a laser is used to propel material from a donor substrate onto a receiving platform (Barron et al. 2004; Ovsianikov et al. 2010). Similar to inkjet printing, small droplets of bioink (down to femtoliters) are transferred from donor to receiver (Koch et al. 2012). However, in comparison to inkjet printers, laser-assisted bioprinters are capable of much higher cell densities (on the order of 100,000,000 cells/mL) as well as a wide range of viscosities (Koch et al. 2012). In contrast, these types of printers are significantly more expensive (Murphy and Atala 2014).

Extrusion (or micro-extrusion) bioprinters use pressure to extrude continuous strands of bioink onto a platform. Like inkjet printing, it has become common for many groups to build their own bioprinters, indicating the ease of using this type of printer. One trait of extrusion bioprinters is that they shear the material during the printing process as the material is forced through a needle. As a result, care must be taken to ensure cells remain viable, as numerous factors, including pressure, needle size, and rheological properties of the material, can lead to low cell viabilities (<50%)

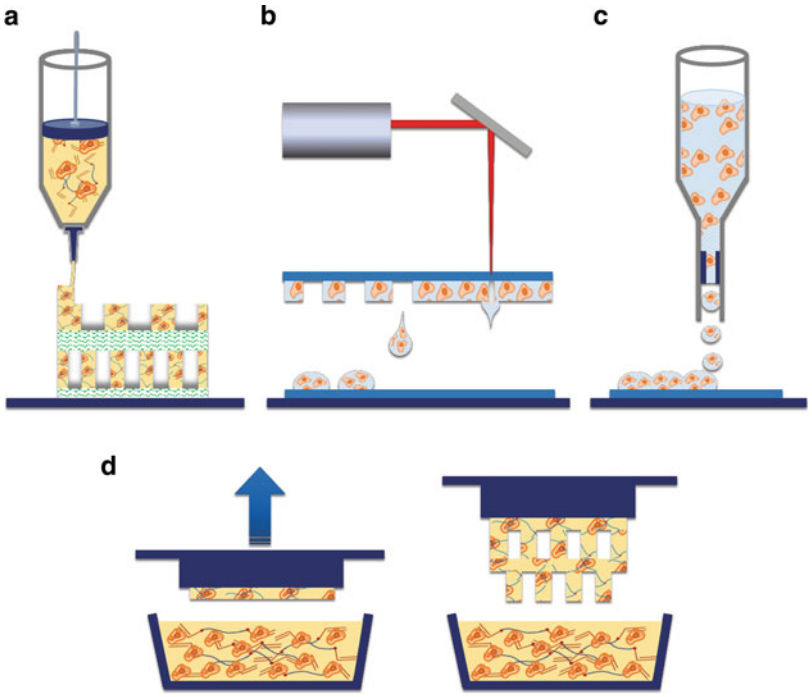

Fig. 1 Schematic of 3D printing methods for cell-laden hydrogels. There are several available 3D printing methods which can be used for cell-laden hydrogels. (**a**) Extrusion printing. Extrusion 3DP entails the use of pressure to extrude continuous strands of bioink onto a platform. Shown here, a piston applies force to cell-laden material which is extruded onto a platform. Multiple bioink cartridges may be used as shown here where the cell-laden material is *yellow* and a second material is shown in *green* and *white*. (**b**) Laser-assisted bioprinting (LAB). LAB uses laser diode and a mirror to direct the laser onto specific points of a platform. The laser contacts a laser-sensitive material which results in the release of the cell-laden material onto a collection platform. (**c**) Inkjet Printing. Inkjet bioprinters function using thermal or piezoelectric forces (*dark blue plates* within the nozzle) to dispense droplets of bioink onto a platform. (**d**) Stereolithography (SLA). SLA printing entails projection of a light source through a specially designed mask to crosslink material one layer at a time. In the setup depicted here, the platform moves upward as each layer is crosslinked and added onto the structure

(Yu et al. 2013). In addition, they are comparatively slow and tend to have lower resolution than inkjet or laser-assisted bioprinters since continuous strands, not droplets, are being deposited (Murphy and Atala 2014).

Stereolithography (SLA) is a less frequently used approach for 3DP of cell-laden hydrogels (Melchels et al. 2010). In this method of 3DP, cell-laden gel solutions are selectively crosslinked according to an image mask or by scanning laser beam layer by layer with ultraviolet (UV) light, or visible light using a projector and digital light processors (DLP) (Melchels et al. 2010). The use of SLA for printing hydrogels implies the need for photo-crosslinkable polymers and as such limits the materials which may be used in this application (Melchels et al. 2010). Moreover,

photo-crosslinkable polymers can entail exposure of cells to potentially harmful UV radiation, and careful selection of photoinitiators is necessary to minimize harm to cells (Bryant et al. 2000; Melchels et al. 2010). Finally, SLA approaches to encapsulate cells require the use of a high volume of cell-laden working solution, which is both expensive and time consuming (Melchels et al. 2010; Lin et al. 2013). Nonetheless, several groups have demonstrated the ability to generate cell-laden, layered constructs with complex geometries and viable cell populations (Dhariwala et al. 2004; Mapili et al. 2005; Arcaute et al. 2006; Chan et al. 2010; Lin et al. 2013).

In comparing the four types of printers, and the body of current literature, it is clear that inkjet and extrusion bioprinters are dominant for hydrogel bioprinting. Both are capable of reaching high cell viability with cell densities comparable to that of traditional hydrogel fabrication methods, both can be used with a wide variety of materials, and, importantly, both are inexpensive and relatively easy to build using off-the-shelf parts. In fact, numerous groups have built their own inkjet or extrusion bioprinters (Yan et al. 2005; Lee et al. 2009, 2014; Cui et al. 2012; Xu et al. 2013a; Melchels et al. 2014; Xu and Wang 2015). Thus, both provide options for beginning to bioprint hydrogels and can be made more complex later on to increase the complexity of printed constructs. While LAB and SLA offer some advantages over inkjet and extrusion printers, such as handling higher viscosity materials and generally having higher cell viability, these have yet to be used to fullest capability. For example, LAB may be used in printing complex tissues, such as the placenta, bone tissue, or lymph nodes, with high cell densities to make improved in vitro models for understanding cell-cell interactions and bulk properties of the tissue. Figure 2 provides a flow chart to aid in choosing the right type of bioprinter.

Resolution of a printed gel often is dependent upon the printer, which could impact the choice of bioprinter needed. Both inkjet printers and laser-assisted bioprinters are limited by the size of the droplet being transferred while extrusion printers are limited by the needle size. These are technological limitations. However, resolution is also dictated by material used. Highly viscous materials, for example, may not be capable of being transferred or extruded using the smallest size droplet or needle. Cells within the bioink may also limit resolution. For example, inkjet printing small droplets at a high cell density may result in cells being sheared, and possibly dying, as they fall onto the platform surface, as may be a similar case for trying to extrude large cells through a small needle in an extrusion bioprinter. Further, resolution is important to consider in the context of the desired end goal. For example, the resolution desired in printing biologically active molecules may be different than the resolution needed to print the scaffold without biological additives. Thus, both bioink composition and printer resolution should be considered when considering the resolution of bioprinters.

2.2 Mechanical Support and Printability

The key aspect of 3DP is the ability to control the overall structure and microarchitecture of the final, printed product. Here, we will refer to that control as "printability." If a material or design is printable, then the accuracy of fabricated

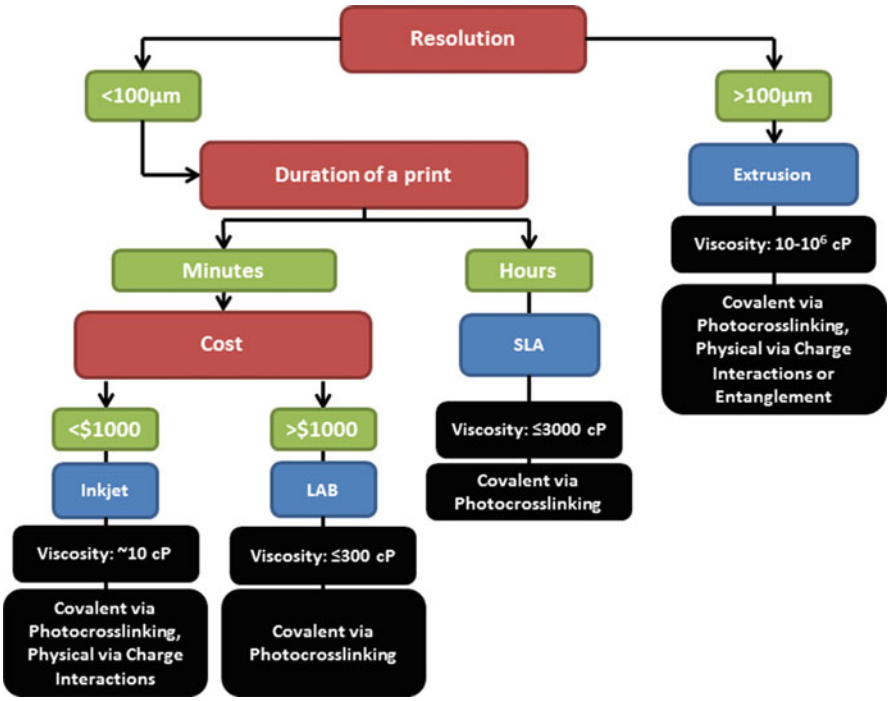

Fig. 2 Flow chart for choosing a bioprinter. The four primary types of bioprinters vary in achievable resolution, duration of a print (the time from start to finish), cost, capable viscosities, and methods of crosslinking polymers that can be used with the 3DP. To aid in choosing a printer, these key factors are broken down. *Red boxes* indicate a decision that must be made, *green boxes* indicate options for that decision, *blue boxes* indicate printer choices, and *black boxes* indicate details related to the printer choice. For example, extrusion printers offer the lowest resolution but can print the highest viscosity bioinks and offer the widest range of polymer crosslinking methods. Inkjet, laser-assisted bioprinters, and stereolithography (SLA) all offer better resolution and can be further chosen based upon duration of a print and cost

product with regard to theoretical and intended design will be high. While printability is often considered largely driven by design, it is also driven by the bioink and material being used. In some cases, it is necessary to use a support material that can later be sacrificed in order to get the final, desired structure (Kolesky et al. 2014; Hinton et al. 2015). These sacrificial materials help support architectural features within the design that are intended to be surrounded by open space. This is a common approach in trying to create vascularized tissue constructs, where sacrificial materials are used during the printing process, evacuated post-printing to create channels, and those channels later seeded with endothelial cells (Kolesky et al. 2014; Bertassoni et al. 2014b). In addition to support materials, printability is also determined by the viscosity of the bioink itself.

Natural polymers, meaning polymers (or their products) commonly derived from an organism, tend to be widely used in bioprinting. However, sometimes their

viscosity presents an issue in the printing process (Shim et al. 2012; Kolesky et al. 2014). This is particularly true for hydrogels, since gelation is based upon the viscosity of the material. A sharp increase in viscosity generally indicates that gelation has occurred. Two materials commonly used in bioprinting that exhibit different viscosities depending on exogenous variables are gelatin and alginate. Gelatin is similar to its precursor, collagen, in that both exhibit temperature-dependent rheological properties (Pietrucha 2005; Florián-Algarín et al. 2008). Thus, bioink formulations that use gelatin as the polymer may need to be printed at a temperature that allows the ink to be viscous enough to print and not spill as a liquid, yet not so viscous as to prevent the material from being printed (Kolesky et al. 2014). Alginate is another natural polymer; however, it exhibits shear-dependent rheological behavior (Rezende et al. 2009). As a result, printing alginate may require some optimization in order to get an appropriate fluid viscosity, with or without a support structure, such that the bioink becomes printable (Shim et al. 2012). Thus, in hydrogel printing, it is important to consider the viscosity of the bioink to ensure that it will be printable, as well as taking into account any support structure that will be needed to achieve an intended design.

2.3 Stress in Cell-Laden Hydrogels

As alluded to previously, bioprinting of cell-laden hydrogel bioinks exposes cells to stress atypical of traditional methods of fabricating hydrogels. In LAB and inkjet printing, cells are exposed to shear stress as strands are extruded out of the needle. Finally, while stereolithography overcomes the limitation of shear stress introduction, cells undergo other stresses as a result of this fabrication method. Potentially harmful stresses associated with can include exposure to UV and photoinitiator chemicals associated with crosslinking the hydrogels and discussed in depth in the next section. Recently, a few studies have looked at how printing impacts cell viability.

A study by Xu et al. was among the first to show inkjet printing is capable of keeping mammalian cells alive (Xu et al. 2005). In this study, Chinese hamster ovary (CHO) cells were suspended in 3× Dulbecco's PBS at a concentration of 5,000,000 cells/mL and printed onto soy agar or collagen. They modified a Hewlett-Packard desktop printer (HP 550C) and HP ink cartridge (51626a) to print their cell suspensions. They compared cell death as a function of bioink formulation and printing processing. They found that, on average, 3.3 ± 3.7% of the cells lysed as a result of the printing process compared to the 18.6 ± 3.7% cells lysing due to bioink formulation. This indicated that the vast majority of the cells were able to live, regardless of the potential damage done by the inkjet printing process. Others have evaluated similar parameters for extrusion-based bioprinters (Nair et al. 2009; Yu et al. 2013; Blaeser et al. 2016).

In a study done by Blaeser et al., cells were exposed to varying levels of shear stress, which was then correlated with the cell viability (Blaeser et al. 2016). Using L929 mouse fibroblast cells encapsulated in alginate, prints were conducted in three

experimental groups, based upon shear stress: lower than 5 kPa, between 5 and 10 kPa, and greater than 10 kPa. The lowest shear stress group (<5 kPa) resulted in 96% cell viability, indicating minimal impact on the overall cell population. However, viability decreased to 91% for the middle group (shear stress between 5 and 10 kPa) and 76% for the higher group (shear stress >10 kPa), indicating an inverse correlation between shear stress and cell viability. A similar correlation was obtained with human mesenchymal stem cells (hMSCs), where cells were 94% viable for a shear stress of 4 kPa, 92% for 9 kPa, and 86% for 18 kPa. This group further investigated the impact of shear stress on cells by evaluating cell function after exposure to printing-associated shear stress. Again, using hMSCs and low (<5 kPa), medium (5–10 kPa), and high (>10 kPa) shear stress experimental groups, cell-laden hydrogels were stained for vimentin, an intermediate filament mesenchymal marker, and CD34, an endothelial marker, and showed no change in phenotype over the course of 7 days. Other groups have looked at cell viability as a function of printing parameters, such as nozzle size, and found that parameters that would increase shear stress, such as small needles or higher printing pressures, resulted in more cell injury or cell death (Nair et al. 2009; Yu et al. 2013). One study done by Zhao et al. looked at the impact of holding time, meaning how long a bioink was held at set conditions prior to printing, and temperature on cell viability (Zhao et al. 2015). In this study, longer holding times and lower temperatures resulted in significantly lower cell viability (in some cases down to 72%), indicating that some printing parameters are significantly more important than others when considering the impact on cell viability and functionality post-printing.

3 Methods for Polymer Crosslinking

In bioprinting hydrogels, one aspect that is fundamental to the printability of a bioink is the method for crosslinking the polymer. There are a few common methods for crosslinking a polymer, but not all of them may be amenable to bioprinting. The simplest method, in terms of printing, is photo-crosslinking initiated by ultraviolet (UV) or visible light, whereby polymer chains are covalently bonded together. Temperature-induced gelation of hydrogels can also be utilized as a method for solidifying materials. Lastly, hydrogels may also be ionically crosslinked, whereby molecular interactions maintain structural integrity. Here we will consider how each method affects the bioprinting of cells with a summary of the mechanisms depicted in Fig. 3.

3.1 Photo-crosslinking

Photo-crosslinking is commonly used because it can rapidly crosslink a large hydrogel. Briefly, photo-crosslinking uses a photoinitiator to create a free radical within the polymer network. This radical rapidly penetrates throughout the network, causing chemical bonds to form between neighboring polymer chains until

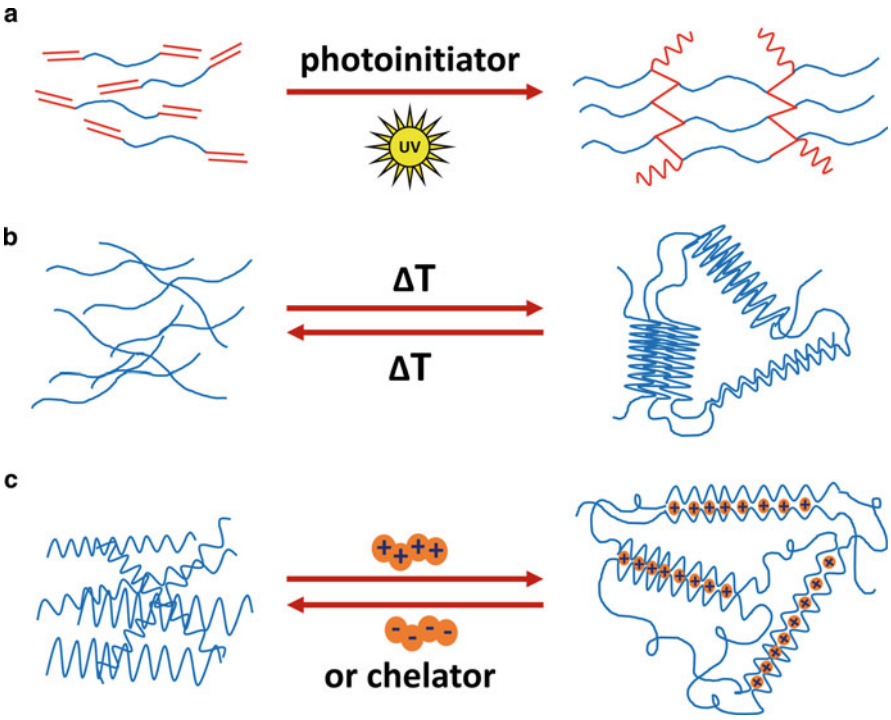

Fig. 3 Methods for generating hydrogel networks. Hydrogels may form networks through both physical and chemical interactions which can be reversible or permanent. (**a**) Photo-crosslinking uses a photoinitiator coupled with a light source (such as UV shown here) to generate free radicals. The free radicals rapidly propagate throughout the network, causing chemical bonds to form between the susceptible moieties of neighboring polymer chains (depicted in *red*). (**b**) Temperature-dependent physical entanglement occurs when materials exhibit thermoreversible gelation, with the bulk material solidifying at low temperatures and liquefying at higher temperatures. (**c**) Ionic crosslinking entails the use of charged compounds (depicted in *orange*) as crosslinkers to create ionic interactions between sites exhibiting the opposite net charge of the crosslinkers. These interactions may be reversed with oppositely charged particles or chelators

the free radicals can no longer propagate. While this method can successfully maintain the structure of the printed gel, it can lead to problems in terms of cell viability. Radical initiators, extended exposure to UV light, and the power of UV irradiation may lead to a decrease in cell viability (Rouillard et al. 2011; Mironi-Harpaz et al. 2012; Billiet et al. 2014). In spite of these concerns, photo-crosslinking is still rapid and can yield cell viabilities that are sufficient for many applications (Rouillard et al. 2011; Billiet et al. 2014). Further, photo-crosslinking allows for control over the rate and degree of crosslinking, allowing for more controlled design of the hydrogel (Skardal et al. 2010).

In some cases, materials are functionalized in order to add groups that can undergo a radical reaction to enable photo-crosslinking of the hydrogel network.

One common example of this is the addition of acrylate or methacrylate groups to the polymer backbone. This has utilized with gelatin (Skardal et al. 2010; Schuurman et al. 2013; Bertassoni et al. 2014a; Billiet et al. 2014; Gao et al. 2015a), hyaluronic acid (Skardal et al. 2010; Duan et al. 2014), poly(ethylene glycol) (Ovsianikov et al. 2010; Cui et al. 2012; Hockaday et al. 2012; Hong et al. 2015; Gao et al. 2015b), and polyvinyl alcohol (PVA) (Schmedlen et al. 2002). These materials are biocompatible and support cell growth and proliferation on their own. Thus, functionalization provides the advantages of their inherent properties with the added benefit of having significantly better control over crosslinking.

Free radical-mediated photo-crosslinking or photopolymerization of a given material requires the presence of a photo-crosslinkable functional group and a photoinitiator (Andrzejewska 2001; Ifkovits and Burdick 2007). The selection of initiators must be carefully considered when bioprinting hydrogels in order to optimize cell viability and printed construct mechanical and physical properties (Bryant et al. 2000; Williams et al. 2005; Pereira and Bártolo 2015). In particular, light radiation and the presence of free radicals and unreacted double bonds can be detrimental to cell viability (Bryant et al. 2000; Williams et al. 2005; Wallace et al. 2014). To reduce damage from such factors, it is important to choose an efficient and minimally cytotoxic photoinitiator wherein light intensity and exposure time can be minimized (Pereira and Bártolo 2015). This can be achieved by closely matching the photoinitiator absorption spectra to the emitting light source wavelength and further by selecting a photoinitiator with cytocompatibility throughout the reaction process (Bryant et al. 2000; Andrzejewska 2001). A handful of commercially available photoinitiators have been found to be cytocompatible for use with a variety of cell types including 2-hydroxy-1-[4-(hydroxyethoxy)phenyl]-2-methyl-1-propanone (Irgacure 2959), lithium phenyl-2,4,6-trimethylbenoylphosphinate (LAP), and riboflavin (Bryant et al. 2000; Williams et al. 2005; Hu et al. 2012; Chen et al. 2012; Li et al. 2015; Davey et al. 2015; Ahearne and Coyle 2016). In stereolithography applications, undesirable free radical propagation can extend beyond the illuminated area intended to be crosslinked, negatively impacting feature resolution, crosslinking density, and subsequently impacting mechanical properties (Elomaa et al. 2011; Wallace et al. 2014; Wang et al. 2015b). The addition of photoinhibitors and absorbing dyes has been shown to mitigate these concerns in cell-free photo-crosslinking applications (Melchels et al. 2009; Elomaa et al. 2011; Wallace et al. 2014). Photoinhibitors such as vitamin E and hydroquinone prevent premature crosslinking by quenching free radicals (Melchels et al. 2009; Elomaa et al. 2011; Wang et al. 2015a). The addition of dyes or pigments such as Orasol Orange G, 2-hydroxy-4-butanoic acid (HMB), and titanium dioxide blocks penetration of radiation to prevent undesired radical generation and crosslinking (Elomaa et al. 2011; Wang et al. 2015b). Unfortunately, while several photoinitiators have been shown to be cytocompatible, to the best of the authors' knowledge, the use of inhibitors and dyes in cell-laden bioprinting has not been investigated, indicating the need for further work in this area (Wallace et al. 2014).

3.2 Thermal Crosslinking

Temperature-induced gelation is another method for crosslinking materials, though it is limited by the material and the printer. In terms of materials, gelatin is a commonly used material that exhibits thermoreversible gelation, with the bulk material solidifying at low temperatures and liquefying at higher temperatures (Hinton et al. 2015). In terms of printers, extrusion-based printers are generally the only type capable of printing a material that can later be crosslinked by temperature (Smith et al. 2007; Khalil and Sun 2007).

In addition, there is a limitation in terms of gelation kinetics. As previously discussed, printing hydrogel materials requires that the bioink be sufficiently viscous to maintain its structure as printing occurs. After completion of the printing process, a structure is generally allowed for fully undergo crosslinking – here that means that the structure would be placed at an appropriate temperature to allow a complete transition to the solid state. However, thermal gelation often occurs at a rate that is too low in order to both maintain an appropriate viscosity for printing and be viscous enough to maintain its structure during the printing process (Moraes et al. 2013; Tsai et al. 2015; Lee et al. 2016). In addition, allowing gelation to occur within the syringe for too long may clog the printer tip due to the increased viscosity of the bioink and the lower temperature of the printer tip, compared to the syringe (Hinton et al. 2015). A recent study found it took 170 s in order to fully gel a novel, thermo-responsive polyurethane, which may still be too long, leading to difficulty in the printing process (Tsai et al. 2015). However, this is still notable as being relatively quick compared to other polymers. Collagen, for example, generally takes 30 min at 37 °C to fully gel (Moraes et al. 2013; Lee et al. 2016). As a result, those who have printed collagen have needed a framework in order to maintain the structure of the collagen (Lee et al. 2016). In general, thermo-responsive polymers have been difficult to print due to the slow gelation kinetics. Thus, this is an area in need of novel approaches, such as synthesizing new polymers with improved gelation kinetics (Tsai et al. 2015).

3.3 Ionic Crosslinking

Ionic crosslinking uses charged compounds to create crosslinks within a polymer network. The most common example of this is alginate, wherein calcium chloride is commonly used as the crosslinker (Song et al. 2011; Shim et al. 2012; Yu et al. 2013; Hong et al. 2015). In this system, alginate chains interact with calcium ions to form a polymer network. In bioprinting, different methods have been used when crosslinking alginate. Shim et al. used an extrusion system to create a support structure, deposit alginate, and later crosslink the alginate using calcium chloride, in the presence of sodium chloride, for 10 min (Shim et al. 2012). In contrast, Yu et al. used a coaxial nozzle system in an extrusion printer (Yu et al. 2013). In this system, the biomaterial and the crosslinker solution were kept at different flow rates, but began to mix at the tip of the needle or the interface where the needle meets the

printing platform. This "double-barrel" style of syringe allowed for controlled printing without the need for later crosslinking via solution. Alginate has also been used in an inkjet-style printer. Faulkner-Jones et al. created a system that dispensed nanoliters of printing solution onto a platform (Faulkner-Jones et al. 2015). Here, an alginate solution and calcium solution were printed next to each other, with crosslinking occurring at the interface of the two solutions. This indicates feasibility of using this crosslinking method in multiple types of bioprinters. Further, while this mechanism has primarily been used for alginate, chitosan is another polymer that has been extensively used and can ionically crosslink, indicating potential for chitosan to become useful as a bioprintable material in future applications (Berger et al. 2004).

4 Multi-material Hydrogel Printing

By this point, it should be clear what the major challenges are in bioprinting cell-laden hydrogels, common methods for addressing some of these challenges, and limitations that stem from the fundamental biology and chemistry of the intended system. Here, we explore selection of an appropriate material, discuss some commonly used materials, and showcase examples of how these materials interact in multi-material printing of hydrogels.

4.1 Material Selection

A key aspect of hydrogel bioprinting is determining which material will be used for printing. Up to this point, we have mainly discussed applications using gelatin, hyaluronic acid, PEG, and alginate (Skardal et al. 2010; Hockaday et al. 2012; Duan et al. 2013; Hinton et al. 2015; Hong et al. 2015; Gaetani et al. 2015; Zhao et al. 2015). The benefits of these materials include, but are not limited to, biocompatibility, functionalization capacity, and ease of crosslinking into a gel. However, there are other materials which have been shown to successfully generate cell-laden hydrogel scaffolds. Examples of commonly used materials will be discussed in detail later, but some other less commonly used include fibrin or fibrinogen (Lee et al. 2010; Xu et al. 2013a; Xu and Wang 2015), gellan gum (GG) (Melchels et al. 2014; Levato et al. 2014), Pluronic F127 (Smith et al. 2004; Kolesky et al. 2014; Müller et al. 2015), polyurethanes (Hsieh et al. 2015), PVA (Schmedlen et al. 2002), and decellularized tissue (Pati et al. 2014, 2015). Each of these materials has unique benefits, which ultimately dictates why they may be chosen over other materials for a given application. For example, fibrin is the polymerized form of the protein fibrinogen that is a part of the blood coagulation cascade and thus can be a good environment for endothelial cells to spread and proliferate. Another example is the use of GG, which has been shown to increase the viscosity of the bioink to help improve its printability (Melchels et al. 2014). Ultimately, in each investigation described herein, materials were chosen with a particular end goal in mind. The question thus becomes: What should be considered when choosing a material?

As in choosing a bioprinter, each material has its advantages and disadvantages. The first question is whether to use a natural polymer or a synthetic polymer. Natural polymers are advantageous due to their biocompatibility, yet often have the drawback of weak mechanical properties (Gao et al. 2015a; Kundu et al. 2015). In addition, the intrinsic crosslinking method of a natural polymer may cause printing to be difficult. In contrast, synthetic polymers are easy to process and/or modify, yet may be cytotoxic to cells (Murphy and Atala 2014). While the vast majority of hydrogels used in bioprinting applications are composed of natural polymers (Fedorovich et al. 2008; Rutz et al. 2015; Ouyang et al. 2015a; Tabriz et al. 2015; Pereira and Bártolo 2015), there have been examples where synthetic polymers were used (Visser et al. 2013; Zhang et al. 2015). Beyond just the broad material classification, further rationale is needed for selection of a material. This includes consideration of a material's mechanical properties and how that may affect the cells embedded, the presence of binding sites, and the ability of cells to spread and adhere to the material, as well as the printability of the material. Fibronectin, for example, is commonly employed to enhance cell adhesion, yet has not been widely used as the primary material for bioprinting (Fedorovich et al. 2011). Poly(2-hydroxyethyl methacrylate), or pHEMA for short, has been commonly used in various applications, such as for soft contact lenses (Galante et al. 2015; García-Millán et al. 2015), but is less commonly used in 3DP applications (Hanson Shepherd et al. 2011; Mohanty et al. 2016). The sparse use of materials such as fibronectin and pHEMA is in contrast with the numerous alginate applications, including both extrusion and inkjet bioprinting (Song et al. 2011; Shim et al. 2012; Pataky et al. 2012; Yu et al. 2013; Faulkner-Jones et al. 2015; Markstedt et al. 2015). Thus, the extent of existing literature and expertise with a material should inform the material selection in bioprinting cell-laden hydrogels. Materials and some of their properties are outlined in Fig. 4 to aid in material selection.

One interesting avenue that is emerging both in the broader context of tissue engineering and more specifically within hydrogel bioprinting is the use of decellularized tissue (Pati et al. 2014, 2015). In essence, the bioink is formed from whole tissue that has, as the name implies, the cells removed, leaving only the extracellular matrix (ECM). The ECM is then solubilized to form a viscous solution for the bioink. Fundamentally, using decellularized tissue ECM as the material for printing provides a significantly enhanced biomimetic environment for encapsulated cells, in terms of material composition. Specifically, ECM proteins are rich in cell adhesion moieties such as GFOGER and RGD peptide sequences found in triple helical collagen and fibronectin, respectively (Petit and Thiery 2000; Hynes 2002; Takada et al. 2007). Studies have also shown enhanced tissue-specific cell differentiation through the use of ECM derived from the tissue of interest (Pati et al. 2014). In these studies, the primary bioink materials investigated were decellularized adipose, cartilage, and heart tissues. As a supportive material, to help with maintaining the structural integrity of the printed hydrogel, polycaprolactone (PCL) was used as a framework. The investigators first looked at differentiating human adipose-derived stem cells (hASCs) and human inferior turbinate tissue-derived mesenchymal stromal cells (hTMSCs) toward chondrogenic (cartilage)

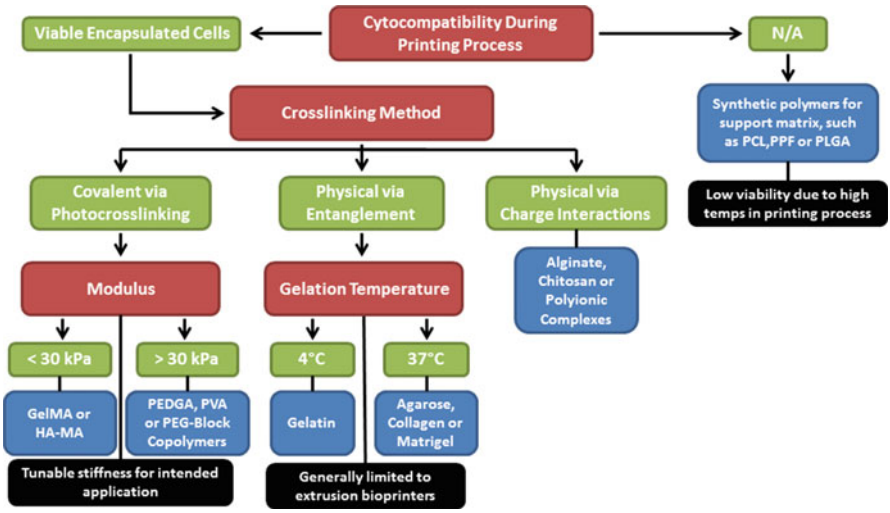

Fig. 4 Flow chart for choosing a material. Material selection can be informed by cytocompatibility during the printing process, method of crosslinking the polymer, mechanical properties, and, in the case of entangled polymers, gelation temperature. *Red boxes* indicate a decision that must be made, *green boxes* indicate options for each decision, *blue boxes* indicate the resulting materials, and *black boxes* indicate comments related to a decision or material. For example, wanting a highly cytocompatible material that can be thermally crosslinked at 37 °C indicates that agarose, collagen, or Matrigel should be used. In addition, the use of thermally crosslinked polymers is generally limited to extrusion-based bioprinters, thus limiting the choice of 3DP

and adipogenic (fat) lineages (Pati et al. 2014). Interestingly, they found that the decellularized tissue associated with each of those lineages enhanced the cellular differentiation, indicating the benefit of using tissue-specific ECM. In a later study, the group sought to see if printed constructs using adipose tissue ECM supported fat tissue growth (Pati et al. 2015). They decellularized adipose tissue, printed dome-shaped constructs using the material, and ultimately implanted the constructs into mice. The group found that the constructs did not cause inflammation and supported formation and constructive remodeling of the tissue. This recent work indicates the potential for using decellularized tissue as the primary material in bioink formulations for bioprinting hydrogels that can advance the field of tissue engineering and regenerative medicine.

4.2 Common Materials in Hydrogel Bioprinting

Hydrogel bioprinting has been investigated for over a decade (Barron et al. 2004; Xu et al. 2005). This longevity might imply the field has advanced to using a vast selection of materials, yet literature shows only a handful are regularly used. As previously mentioned, four of the most commonly used materials are (1) alginate (Cohen et al. 2010; Song et al. 2011; Shim et al. 2012; Fedorovich et al. 2012; Pataky

Table 1 Common materials used in hydrogel bioprinting. Alginate, GelMA, HA-MA, and PEGDA are among the most commonly used materials in bioprinting hydrogels. Key characteristics of these materials include their mechanical properties, cell compatibility, mechanisms for crosslinking, printers that have been used with each material, and their associated resolution

Material	Mechanical properties	Cell compatibility	Crosslinking methods	Printers	Resolution
Alginate	Elastic modulus: 5–30 kPa	75–96% viability	Ionic	Inkjet, extrusion, laser	10–100 μm (inkjet), 320–640 μm (extrusion) , 500 μm (laser)
Gelatin methacrylate (GelMA)	Modulus: 3–60 kPa	60–90% viability	Photo-initiated, thermal	Inkjet, extrusion	150–200 μm
Hyaluronic acid methacrylate (HA-MA)	Modulus: 4–12 kPa	>90% viability	Photo-initiated	Extrusion	<1 mm
Poly (ethylene glycol)-diacrylate (PEGDA)	Compressive modulus: 30–395 kPa	90% viability	Photo-initiated	Inkjet, extrusion	20–85 μm (inkjet), 500 μm (extrusion)

et al. 2012; Yu et al. 2013; Zhang et al. 2013; Faulkner-Jones et al. 2015; Tabriz et al. 2015; Blaeser et al. 2016), (2) gelatin (Schuurman et al. 2013; Bertassoni et al. 2014a; Billiet et al. 2014; Melchels et al. 2014; Ma et al. 2015), (3) hyaluronic acid (Skardal et al. 2010; Duan et al. 2014; Highley et al. 2015; Kesti et al. 2015), and (4) poly(ethylene glycol) (PEG) (Cui et al. 2012; Hockaday et al. 2012; Hong et al. 2015; Ma et al. 2015; Gao et al. 2015a). Some characteristics of these materials are outlined in Table 1. Here, we will elaborate on studies involving each of these materials more in depth.

Alginate is perhaps the most common material used in hydrogel printing and has been shown to work using both inkjet printers and extrusion-based printers (Pataky et al. 2012; Faulkner-Jones et al. 2015; Sher et al. 2015; Tabriz et al. 2015). Alginate is biocompatible, is non-immunogenic, can be crosslinked in a reversible and controlled manner, and can form highly porous structures that support cells (Faulkner-Jones et al. 2015; Tabriz et al. 2015). As previously discussed, alginate crosslinks through the use of calcium ions that cause chains of alginate to interact, with strong enough interactions to result in the formation of a hydrogel network (Yu et al. 2013; Hong et al. 2015). In printing alginate, multiple approaches have been taken. In one method, an inkjet-style printer was used to print an alginate solution followed by a calcium solution, thus allowing for crosslinking to occur at the interface (Faulkner-Jones et al. 2015). Another approach using an inkjet printer was to embed calcium ions into a gelatin-based gel substrate and allow for the

diffusion of calcium ions from the substrate to crosslink the alginate as it is being deposited on top (Pataky et al. 2012). An interesting approach taken by Tabriz et al. used a modified Fab@Home extrusion printer to print cell-laden alginate onto a substrate that was on a z-axis controlled platform (Tabriz et al. 2015). As the printing continued, the platform would move downward into a solution of calcium chloride-enriched culture media. Interestingly, this method would allow for continuous crosslinking of the bottom portion of the structure, perhaps leading to a mechanically enhanced structure, assuming alginate chains are still available for crosslinking. Other groups have also printed alginate solutions into a calcium solution in order to crosslink their hydrogels (Blaeser et al. 2016). In addition to variability in crosslinking approaches used, the concentration of alginate has varied in applications from 0.5 to 6% w/v (Zhang et al. 2013; Blaeser et al. 2016). These differences have been shown to impact cell viability and solution viscosity (Yu et al. 2013; Blaeser et al. 2016), indicating a need to optimize the composition of the alginate bioink for its intended application.

Gelatin is another commonly used material that is biocompatible, is biodegradable, and exhibits thermoreversible gelation (Schuurman et al. 2013). Gelatin naturally gels at low temperature and liquefies at high temperature. Some groups have used unmodified gelatin (Ouyang et al. 2015b; Zhao et al. 2015), while others have functionalized gelatin, most commonly by adding methacrylate groups (Schuurman et al. 2013; Bertassoni et al. 2014a). When using unmodified gelatin, efforts were made to ensure printing occurred within the temperature range for gelation to occur (Ouyang et al. 2015b; Zhao et al. 2015). While this approach ensures integrity of the bioink and the printed structure throughout the printing process, using unmodified gelatin may lead to degradation of the hydrogel during the growth and culture of cells at 37 °C. Interestingly, one study using a gelatin-alginate hydrogel found that cell growth continued in patterns mimicking the initial printed structure, showing it may be possible to maintain a printed design when combining gelatin with another material (Ouyang et al. 2015b). In contrast, functionalized gelatin, specifically methacrylated gelatin (GelMA), can form a hydrogel network through photocrosslinking. GelMA provides the benefits of gelatin along with the capacity for rapid and controlled polymerization. Bioinks using gelatin or GelMA have typically used 5–20% w/v within the final bioink formulation (Schuurman et al. 2013; Bertassoni et al. 2014a; Zhao et al. 2015). One study showed that the compressive modulus of GelMA hydrogels varied depending on gelatin concentration and gelation temperature. Their work illustrated that 10% w/v and 20% w/v GelMA had a modulus of 30–50 kPa and 200–300 kPa, respectively, when crosslinked at 37 °C or room temperature (Schuurman et al. 2013). These examples serve to showcase the wide range of material properties which can be achieved with gelatin-based bioinks which have resulted in the wide use of these materials in hydrogel bioprinting applications.

Hyaluronic acid (HA), or hyaluronan, is a natural, linear, anionic glycosaminoglycan that is capable of forming a hydrogel network (Pietrucha 2005; Burdick and Prestwich 2011). However, it is less commonly used in bioprinting than either alginate or gelatin, perhaps due to the fact that it is inherently difficult to print

(Burdick and Prestwich 2011). Printing of HA necessitates the use of soluble additives such as dextran to tune the viscosity and functionalization with moieties and proteins to enable crosslinking and enhance cell adhesion (Skardal et al. 2010; Duan et al. 2014). HA network formation is dependent upon functionalization and established mechanisms for functionalizing and crosslinking HA have been thoroughly reviewed (Burdick and Prestwich 2011). A recent investigation by Duan et al. added a methacrylate group to HA, thus making hyaluronic acid methacrylate (HA-MA) (Duan et al. 2014). In this study, the group combined HA-MA with GelMA and found that increasing the HA-MA content from 2% to 6% increased the stiffness of the hydrogel when using 6% GelMA. However, these differences were not apparent using higher amounts of GelMA (10% and 12%). This indicates that HA may be useful as an additive in hydrogels, but may not be the most suitable primary material. This finding was further supported by a group that used HA-MA as a barrier for cell migration, wherein their results indicated that HA-MA did not enable cell adhesion to the matrix without another material present (Skardal et al. 2010). Regardless, HA is a prominent molecule within cartilage tissue and thus may be advantageous for cartilage-focused tissue constructs (Kesti et al. 2015).

Poly(ethylene glycol) (PEG) is a synthetic polymer that has been used in a variety of therapeutic applications approved by the US Food and Drug Administration (FDA) and as such has become increasingly prevalent in translational tissue engineering investigations. Further, PEG is biocompatible and can be easily modified for specific applications (Hockaday et al. 2012). In bioprinting, acrylate-modified PEG, poly(ethylene glycol)-diacrylate (PEGDA), is commonly used to enable photo-crosslinking of the polymer (Cui et al. 2012; Gao et al. 2015a). Furthermore, the mechanical properties of PEGDA are tunable for use in a wide variety of applications (Cui et al. 2012; Hockaday et al. 2012). In using synthetic polymers, such as PEG, not only is polymer concentration important but also the molecular weight (MW) of polymer used. In particular, when using cell-laden hydrogels, the MW of PEGDA can impact cell viability. Specifically, one group showed that MW <3 kDa resulted in decreased viability of encapsulated cells compared with higher MW PEGDA hydrogels (Chan et al. 2010). Using the same polymer with different MW can also yield different bulk material properties. One example of this is that the MW of PEG tends to correlate with the stiffness of the gel, meaning lower MW polymers lead to softer gels (Hockaday et al. 2012). Groups have used PEGDA that ranged from 0.7 to 20 kDa and from 10% to 20% w/v polymer in bioink solution (Cui et al. 2012; Hockaday et al. 2012; Hong et al. 2015; Gao et al. 2015a). In addition, PEG is one of the only materials used in all four major types of bioprinters, truly indicating its versatility (Ovsianikov et al. 2010; Cui et al. 2012; Hockaday et al. 2012; Hong et al. 2015; Gao et al. 2015a).

4.3 Single Bioink Bioprinting

In printing multi-material hydrogels, the use of a single bioink has distinct advantages and disadvantages over the use of multiple, separate bioinks. A depiction of the differences between single and multi-bioinks of homogenous and heterogeneous resins

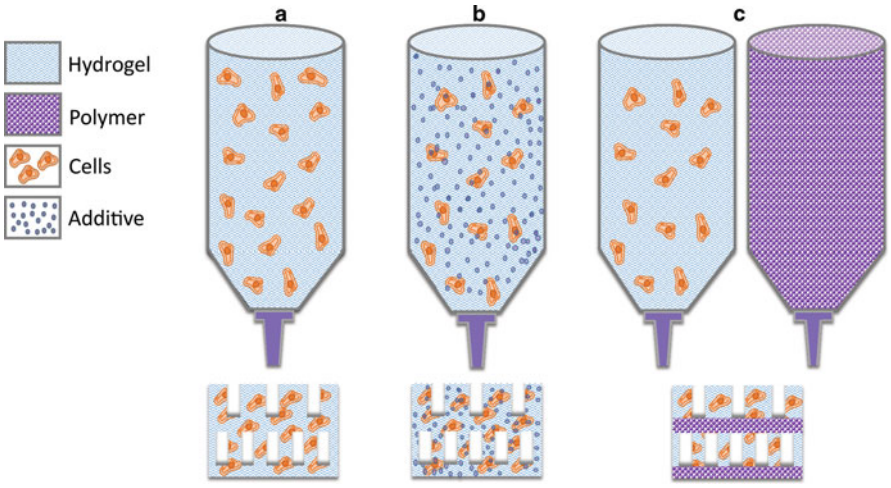

Fig. 5 Single and multi-bioink resins. Multi-material single bioinks benefit cell-laden hydrogel 3D printing by including additives to enhance material viscosity for printing or which can be beneficial to cell viability and target behavior. Cell-laden hydrogels have been printed in a variety of single material hydrogel bioink resins (**a**) and single resins made of multiple materials (**b**). The use of multiple, separated bioinks can benefit 3DP of hydrogels by enhancing the mechanical integrity of printed structures by including stiffer materials such as printable polymers (**c**)

can be seen in Fig. 5. A single bioink will be homogeneous and require only one cartridge. In addition, "hard-to-print" materials can be incorporated into "easy-to-print" materials. For example, hyaluronic acid can be incorporated into a gelatin methacrylate bioink (Skardal et al. 2010). However, using a single bioink prevents the construct from being heterogeneous. This does not prevent investigators from fabricating single bioink constructs for various applications though, as outlined in Table 2.

One set of single bioink examples comes from incorporating GG into a GelMA hydrogel (Melchels et al. 2014; Levato et al. 2014). In two studies, GG was included at a low concentration (0.75–1% w/v) to improve the printing of GelMA. In the study by Melchels et al., they compared the viscosity of four bioinks: (1) 0.75% GG, (2) 10% GelMA, (3) 10% GelMA + 0.75% GG, and (4) 10% GelMA + 0.75% GG + 24 mM cations (Melchels et al. 2014). (To clarify, the 24 mM cations are of any valence and promote the formation of a more brittle GG gel.) Over the range of shear rates tested to investigate the viscosity (0.01–1,000 s^{-1}), they found the GelMA alone and GG alone to be similar, while the combination of both together was generally an order of magnitude higher than either alone. This difference in viscosity was spread even further when including cations, which resulted in nearly an order of magnitude higher viscosity than the combined material and thus two orders of magnitude higher than either material alone (Melchels et al. 2014). In a study done by Levato et al., microcarriers were used in a 10% GelMA/1% GG system to enhance the GelMA matrix that was being printed. Briefly, poly(lactic acid) (PLA) microparticles were coated with collagen and had cells seeded onto them prior to

Table 2 Multi-material hydrogels using a single, homogeneous bioink. Examples of multi-component bioinks are listed here, including the materials used in the bioink; the printer used; the intended application for each material; results of interest, including mechanical properties, and results related to 3DP of the bioink; and the reference information for each study

Materials	Printer	Application	Results of interest	Reference
Agar/acrylamide/alginate	Extrusion	Tough hydrogel	Modulus: 70–870 kPa Strength: 402–1,096 kPa	Wei et al. (2015)
Acrylamide/alginate	Extrusion	Tough hydrogel	Young's modulus: 90–170 kPa Failure strain: 90–300%	Bakarich et al. (2013)
Alginate/collagen	Inkjet	Vascularized bone	Compressive modulus increases to over 2 MPa after 18 weeks implantation, one of the first prints using multiple cell types in a single construct	Xu et al. (2013b)
Alginate/gelatin	Extrusion	Embryoid bodies	>90% cell viability with retention of pluripotent stem cell markers after printing	Ouyang et al. (2015b)
Alginate/gelatin	Extrusion		Storage modulus: 1–100 Pa Loss modulus: 0.1–10 kPa Increased holding time; storage modulus decreased cell viability but increased printability	Zhao et al. (2015)
Alginate/gelatin	Extrusion	Aortic valve	Modulus remains between 0.9 and 1.1 MPa over 7 days of incubation, cell-laden gels have lower moduli than cell-free gels, hydrogel's tensile strength and modulus decrease over time in culture	Duan et al. (2013)

(*continued*)

Table 2 (continued)

Materials	Printer	Application	Results of interest	Reference
Alginate/gelatin/fibrin	Extrusion	Embryonic tissues	Cells maintained function and proliferated within the architecture of the printed	Ouyang et al. (2015a)
Alginate/gelatin/fibrin	Extrusion	Model of energy metabolic system	Cells printed in 3D constructs had higher levels of metabolic activity than those in 2D	Xu et al. (2010)
Alginate/gelatin/fibrin	Extrusion	Cervical tumor model	Observed chemoresistance in 3D printed gels, but not in 2D culture studies	Zhao et al. (2014)
Collagen/fibrin	Inkjet	Cartilage	Young's modulus: 0.77 MPa Combined with electrospun PCL to make a strong scaffold	Xu et al. (2013a)
Gelatin/chitosan	Extrusion	Liver tissue	Showed liver cells maintain some functionality after being printed in a matrix	Yan et al. (2005)
GelMA/GG	Extrusion		Compressive modulus: 15–60 kPa (dose dependent on GG concentration)	Melchels et al. (2014)
GelMA/GG/PLA microcarriers (MCs)	Extrusion	Articular cartilage	Compressive modulus: 27–50 kPa (dose dependent on MC concentration) Cells remained on the surface and did not penetrate into MCs	Levato et al. (2014)
GelMA/HA	Extrusion	Cardiovascular patch	Patches help improve cardiac remodeling after 1 month in vivo	Gaetani et al. (2015)
HA-MA/ adamantane/β-cyclodextrin	Extrusion	Self-healing hydrogels	Printed structures with hollow geometries are self-supporting	Highley et al. (2015)

(*continued*)

Table 2 (continued)

Materials	Printer	Application	Results of interest	Reference
			after removal of support matrix	
HA-MA/gelatin ethanolamide methacrylate	Extrusion	Organ printing	Storage modulus: 10–90 Pa (dependent on crosslinking time)	Skardal et al. (2010)
HA-MA/GelMA	Extrusion	Heart valve	Modulus: 4–12 kPa Increasing GelMA concentration decreased modulus (contrary to most studies)	Duan et al. (2014)
PEGDA/acrylated peptides	Inkjet	Bone and cartilage	Initial compressive modulus: 35 kPa (increased to 50–70 kPa after osteo- or chondrogenesis for 21 days), decreased hMSC hypertrophy in chondrogenic differentiation on scaffolds	Gao et al. (2015b)
PEGDA/alginate	Extrusion	Aortic valves	Modulus: 10–75 kPa (dependent on ratio of MW 700 to MW 8000 PEGDA) Printed constructs 1 cm in size with high cell viability	Hockaday et al. (2012)
PEGDA/alginate/nanoclay	Extrusion	Tough, complex hydrogels	Material returns to nominal shape after relaxation of uniaxial stretching 3× its size or 95% compressive strain	Hong et al. (2015)
PEGDA/GelMA	Inkjet	Bone and cartilage	Initial compressive modulus: 30–40 kPa (increased to 50–70 kPa after osteo- or chondrogenesis for 21 days)	Gao et al. (2015a)

(*continued*)

Table 2 (continued)

Materials	Printer	Application	Results of interest	Reference
PEGDA/GelMA	Inkjet	Periodontal ligament	Saw positive correlation between cell viability and GelMA to PEGDA ratio	Ma et al. (2015)
Silk fibroin/gelatin	Extrusion	Stem cell-laden tissue constructs	Storage modulus: 166–221 kPa (at 37 °C) and 530–751 kPa (at 18 °C) Tyrosinase crosslinked gels had higher moduli and were more stable long term than sonication crosslinked gels	Das et al. (2015)

being mixed in with the GelMA/GG bioink. This provided a dose-dependent mechanical enhancement of the matrix. The compressive modulus for the matrix was 27–28 kPa without microparticles, but increased to over 50 kPa with the addition of microparticles at a dose of 50 mg/mL (Levato et al. 2014). Thus, this system provided a homogeneous bioink that could enhance the mechanical properties of the printed material by using microcarriers, which in itself has potential applications in numerous areas for both growing cells and delivering growth factors. Both studies illustrated the utility of GelMA-GG bioinks in 3DP.

Another system used in several studies is alginate-gelatin combination bioinks (Chung et al. 2013; Duan et al. 2013; Ouyang et al. 2015b; Zhao et al. 2015). This combination is benefitted by the biocompatibility of both materials, the straightforward crosslinking capacity offered by alginate, and the thermo-controllable properties and cell adhesion provided by the gelatin in one system. One study by Zhao et al. sought to characterize the gelation ability of these types of bioinks and the rheological properties at a temperature of 20 °C (Zhao et al. 2015). They found that with minimal changes in alginate concentration (from 0% to 2%), the gelation temperature only minimally changed (from 21 to 22.5 °C). They also found that cell viability was dependent upon the holding temperature, i.e., the temperature at which the bioink was held prior to printing, as well as how long it was held at that temperature. Viability increased with increasing temperatures (from 10 to 20 °C), but decreased with longer holding times (from 5 to 30 min) (Zhao et al. 2015). A similar correlation was found in a study done by Ouyang et al. (2015b). In this investigation, the results showed that cell distribution was well maintained within the printed structure, even though the water-soluble gelatin was not modified to be crosslinkable (Ouyang et al. 2015b). Other studies have also looked at gelatin-alginate hybrids with the addition

of fibrinogen (Zhao et al. 2014; Ouyang et al. 2015a). A system of alginate-gelatin-fibrinogen provides the same benefits as an alginate-gelatin system, but the addition of fibrinogen further helps to stabilize the bioink and may offer an enhanced biomimetic environment through the formation of fibrin from the added fibrinogen (Zhao et al. 2014; Ouyang et al. 2015a). In another study by Ouyang et al., gelatin-alginate and a gelatin-alginate-fibrinogen scaffolds were compared, revealing minor differences in pore size (i.e., the distance between printed strands), thread diameter (i.e., the thickness of a printed strand), and distance between pores (Ouyang et al. 2015a). Hybrid single bioinks, such as the gelatin-alginate and gelatin-alginate-fibrinogen systems described here, have allowed investigators to capitalize on the synergy of material properties, showing potential in a wide range of applications.

4.4 Multiple Bioink Bioprinting

In contrast to a single bioink with multiple materials, multiple bioinks provide more room for complexity in design. Different regions within a single printed construct can be made from a unique bioink, without or without cells, to create localized environments (i.e., a heterogeneous tissue constructs). This provides advantages in engineering complex tissue structures such as interface tissues, wherein multiple microenvironments exist within a single tissue (Fedorovich et al. 2012). In addition, beyond simply printing soft hydrogels, further support materials and structures can be included in order to fabricate constructs with varied mechanical properties, which is advantageous in regenerative medicine applications for hard tissues. Here, we discuss examples of heterogeneous tissue applications, some of which are shown in Table 3.

An example of a multi-material and multi-bioink system is the printing of alginate with PCL (Schuurman et al. 2011; Lee et al. 2013; Kundu et al. 2015; Jung et al. 2016). In these examples, PCL was printed first as a hard material to support the structure of the alginate over the time course of the study (Schuurman et al. 2011; Lee et al. 2013; Kundu et al. 2015; Jung et al. 2016). Initial viability studies of the cells (C20A4, a chondrocyte cell line, and MC3T3-E1, preosteoblast cells) encapsulated in the alginate indicated that approximately 80% of the cells were alive (Schuurman et al. 2011; Lee et al. 2013). Interestingly, this viability decreased over a few days, toward 60%, which the authors hypothesized to be a result of heat shock from the printed PCL cooling (Schuurman et al. 2011). However, the PCL did result in improved mechanical properties of the larger construct. Printing PCL alongside alginate resulted in a higher Young's modulus for the construct (Schuurman et al. 2011; Lee et al. 2013). This method for enhancing mechanical properties of a construct, by providing a hard support structure, enables the printing of difficult to print hydrogel materials. This concept was also demonstrated in a study by Visser et al. in which thermoplastic materials were printed with hydrogels to form mechanically improved structures that better mimicked the anatomically important features of vascular trees and the right ear (Visser et al. 2013). In contrast, there are a handful of studies that have looked at using two different hydrogel materials to fabricate complex 3DP constructs.

Table 3 Multi-material hydrogels using multiple bioinks. Examples of studies that have used multiple bioinks for a single construct are listed here. This includes the materials used, the interactions of the materials, the printer used, the intended application, and results of interest, including mechanical properties, and results related to the use of multiple bioinks, as well as reference information

Materials	Material interactions	Printer	Application	Results of interest	Reference
Alginate/ alginate +biphasic calcium phosphate particles	Two distinct matrices side by side, interfacing on one side	Extrusion	Osteochondral grafts	Modulus: 4.5–15 kPa Saw heterogeneous tissue formation after implanting in vivo in nude mice	Fedorovich et al. (2012)
Gelatin/ ECM mix (collagen type 1/Matrigel/ fibrinogen/ HA)	ECM mix printed into gelatin slurry	Extrusion	Complex biological structures	Printed structures were similar to design parameters, such as the angle between arterial tree branches	Hinton et al. (2015)
GelMA/ Pluronic F127	Sacrificial networks (Pluronic F127) were surrounded by GelMA	Extrusion	Vascularized tissue	Cells in different bioinks only interacted with other cells/ materials at the interface of printed structures	Kolesky et al. (2014)
GelMA/ gellan/ PCL or alginate	PCL or alginate served as a sacrificial matrix for final hydrogel	Extrusion	Model of a distal femur (PCL) of box with tubes (alginate)	Hydrogel constructs were 1–4 cm in length/ width, indicating large constructs could be fabricated	Visser et al. (2013)
Matrigel/ alginate/ biphasic calcium particles	Two distinct matrices side by side, interfacing on one side	Extrusion	Vascularized bone	Saw distinct tissue formation in each matrix after 2 and 6 weeks implantation in vivo	Fedorovich et al. (2011)

One example using multiple hydrogel bioinks comes from a study by Kolesky et al. where the goal was to print a multi-material and multicellular tissue construct with pre-vasculature structures (Kolesky et al. 2014). GelMA (15% w/v) was used as the bulk material, while Pluronic F127 (40% w/v) was printed to later be sacrificed, in order to allow for channels that could later be lined with endothelial cells. Irgacure 2529 was used as a photoinitiator for UV crosslinking of the GelMA at 0.3% w/w in

the bioink. GelMA without cells was used to print the portions of the design that were not meant to contain cells. Cells used in the printing process included C3H/10T1/2 Clone 8 (10T1/2) cells, a fibroblast cell population, from ATCC, and human neonatal dermal fibroblasts (HDNFs) at densities of 2×10^6 cells/mL. Once the Pluronic F127 was sacrificed, human umbilical vein endothelial cells (HUVECs) were injected into the space at a density of 1×10^7 cells/mL. This innovative research illustrated the ability of cells to maintain and localize within a printed structure. In addition, printed gels showed a viability of 60–70% within a day after printing, which continued to increase to approximately 80% by 7 days after printing (Kolesky et al. 2014). This promising and innovative effort further highlighted 3DP technologies as a means for generating complex and multifaceted constructs consisting of multiple materials and cell types. As such, this investigation provides impetus for further investigation of multi-material and multicell hydrogel bioprinting.

One last example is from a study by Fedorovich et al. that aimed to create a heterogeneous scaffold to see if this heterogeneity is maintained after implantation in vivo (Fedorovich et al. 2011). To do this, two cell populations were used – goat endothelial progenitor cells (EPCs) and goat mesenchymal stem cells (MSCs). For materials, BD Matrigel was used to encapsulate EPCs at a density of 5×10^6 cells/mL gel, while MSCs were encapsulated in either alginate or growth factor-depleted Matrigel at a density of 5×10^6 cells/mL gel. The MSC-laden gel also included osteoinductive biphasic calcium phosphate (BCP) microparticles (106–212 μm in size) at 10% w/v to encourage formation of bone tissue. Calcium chloride solution (102 mM) was used to crosslink the alginate, while Matrigel formed a gel at room temperature. As with the vascularized tissue study, this group was able to show that each cell population stayed within the bounds of the printed area of its own bioink, with little to no interactions between the two cell types/materials. For the in vivo portion of the study, the group explanted the scaffolds at 2 and 6 weeks after implantation in subcutaneous dorsal pockets of nude mice and found that the construct maintained its heterogeneity. Blood vessels began to form after 2 weeks within the EPC-laden part of the construct, while bone and cartilage tissue formation were identified in the MSC-laden part of the construct. This study further indicates the promise of heterogeneous 3DP scaffolds by showing the ability of such constructs to be implanted in vivo while maintaining the heterogeneity of the construct.

5 Summary and Future Directions

Bioprinting of hydrogels has made great strides in the last decade. Four major bioprinting modalities have emerged in inkjet bioprinting, extrusion bioprinting, LAB, and SLA. While the former two have become extensively used by various labs with plenty of examples of custom-built bioprinters, the latter two are still in the growth stages and have yet to be fully exploited in their capabilities. Studies have been done to characterize the parameters associated with hydrogel bioprinting, but

more work can be done to further characterize and expand upon these studies for different materials and different cell populations. In addition, research is currently being carried out to better control the crosslinking of various biomaterials by trying new crosslinking methods, as well as attempting to enhance the precise control over thermal and ionically crosslinked polymers (Zhang et al. 2013; Bertassoni et al. 2014a; Highley et al. 2015; Hinton et al. 2015; Zhao et al. 2015). Future work is necessary to investigate modifications to materials which have the potential to provide a useful biomimetic environment, but are presently difficult to print, in order to fully utilize these materials as 3DP bioinks.

For multi-material hydrogels, work has been done evaluating both single, multi-component bioinks and multiple bioinks for generating complex heterogeneous constructs. While much of this work has been done using alginate, gelatin, HA, and/or PEG as the primary polymer, there remain other choices which could enhance the characteristics of the printed constructs. Using other natural polymers, such as collagen, Matrigel, fibrin, or ECM, in combination with synthetic polymers, such as polyurethanes or PEG copolymers, may result in improved printability and, ultimately, regenerative capacity of printed constructs (Fedorovich et al. 2008; Schuurman et al. 2011; Pati et al. 2014, 2015; Rutz et al. 2015; Tsai et al. 2015; Zhang et al. 2015; Hsieh et al. 2015; Lee et al. 2016).

Functionally, little of this work has been translated into the clinic. To date, a therapeutic device consisting of a bioprinted hydrogel construct containing cells, with or without the addition of other growth factors or signals, has yet to be approved by the FDA for clinical application. However, many groups have investigated printed constructs in animal models, indicating the significant progress made toward the goal of clinical translation (Fedorovich et al. 2011, 2012; Xu et al. 2013b; Pati et al. 2015). To this end, it is probable that future work will continue to focus on improved bioprinted tissue functionality with a greater extent of complex approaches being employed such as multicellular heterogeneous tissue constructs and 4D printing.

As it stands, hydrogel bioprinting has become established and continues to move forward, with many groups seeking to expand the limits of current bioprinting capabilities. With continued research in this area, we may find better solutions to existing problems and improve the outlook of the field of 3DP and tissue engineering as a whole.

Acknowledgments This work was supported by a seed grant from the Sheikh Zayed Institute for Pediatric Surgical Innovation at Children's National Medical Center and the A. James Clark School of Engineering at the University of Maryland. Additional funding was provided by the National Science Foundation/US Food and Drug Administration Scholar in Residence Program (CBET1445700). The content is solely the responsibility of the authors and does not necessarily represent the official views of these funding sources.

References

Ahearne M, Coyle A (2016) Application of UVA-riboflavin crosslinking to enhance the mechanical properties of extracellular matrix derived hydrogels. J Mech Behav Biomed Mater 54:259–267. https://doi.org/10.1016/j.jmbbm.2015.09.035

Akkineni AR, Luo Y, Schumacher M, Nies B, Lode A, Gelinsky M (2015) 3D plotting of growth factor loaded calcium phosphate cement scaffolds. Acta Biomater 27:264–274. https://doi.org/10.1016/j.actbio.2015.08.036

Andrzejewska E (2001) Photopolymerization kinetics of multifunctional monomers. Prog Polym Sci 26:605–665. https://doi.org/10.1016/S0079-6700(01)00004-1

Arcaute K, Mann BK, Wicker RB (2006) Stereolithography of three-dimensional bioactive poly (ethylene glycol) constructs with encapsulated cells. Ann Biomed Eng 34:1429–1441. https://doi.org/10.1007/s10439-006-9156-y

Bakarich SE, in het Panhuis M, Beirne S, Wallace GG, Spinks GM (2013) Extrusion printing of ionic–covalent entanglement hydrogels with high toughness. J Mater Chem B 1:4939. https://doi.org/10.1039/c3tb21159b

Barron JA, Ringeisen BR, Kim H, Spargo BJ, Chrisey DB (2004) Application of laser printing to mammalian cells. Thin Solid Films 453–454:383–387. https://doi.org/10.1016/j.tsf.2003.11.161

Berger J, Reist M, Mayer JM, Felt O, Peppas NA, Gurny R (2004) Structure and interactions in covalently and ionically crosslinked chitosan hydrogels for biomedical applications. Eur J Pharm Biopharm 57:19–34. https://doi.org/10.1016/S0939-6411(03)00161-9

Bertassoni LE, Cardoso JC, Manoharan V, Cristino AL, Bhise NS, Araujo WA, Zorlutuna P, Vrana NE, Ghaemmaghami AM, Dokmeci MR, Khademhosseini A (2014a) Direct-write bioprinting of cell-laden methacrylated gelatin hydrogels. Biofabrication 6:024105. https://doi.org/10.1088/1758-5082/6/2/024105

Bertassoni LE, Cecconi M, Manoharan V, Nikkhah M, Hjortnaes J, Cristino AL, Barabaschi G, Demarchi D, Dokmeci MR, Yang Y, Khademhosseini A (2014b) Hydrogel bioprinted microchannel networks for vascularization of tissue engineering constructs. Lab Chip 14:2202–2211. https://doi.org/10.1039/c4lc00030g

Billiet T, Gevaert E, De Schryver T, Cornelissen M, Dubruel P (2014) The 3D printing of gelatin methacrylamide cell-laden tissue-engineered constructs with high cell viability. Biomaterials 35:49–62. https://doi.org/10.1016/j.biomaterials.2013.09.078

Blaeser A, Duarte Campos DF, Puster U, Richtering W, Stevens MM, Fischer H (2016) Controlling shear stress in 3D bioprinting is a key factor to balance printing resolution and stem cell integrity. Adv Healthc Mater 3:326–333

Bryant SJ, Nuttelman CR, Anseth KS (2000) Cytocompatibility of UV and visible light photoinitiating systems on cultured NIH/3T3 fibroblasts in vitro. J Biomater Sci Polym Ed 11:439–457. https://doi.org/10.1163/156856200743805

Burdick JA, Prestwich GD (2011) Hyaluronic acid hydrogels for biomedical applications. Adv Mater 23:41–56. https://doi.org/10.1002/adma.201003963

Carolina N (2012) Bioprinted amniotic fluid-derived stem cells accelerate healing of large skin wounds. Stem Cells Transl Med 1:792–802. https://doi.org/10.5966/sctm.2012-0088

Cha C, Soman P, Zhu W, Nikkhah M, Camci-Unal G, Chen S, Khademhosseini A (2014) Structural reinforcement of cell-laden hydrogels with microfabricated three dimensional scaffolds. Biomater Sci 2:703–709. https://doi.org/10.1039/C3BM60210A

Chan V, Zorlutuna P, Jeong JH, Kong H, Bashir R (2010) Three-dimensional photopatterning of hydrogels using stereolithography for long-term cell encapsulation. Lab Chip 10:2062–2070. https://doi.org/10.1039/c004285d

Chen Y-C, Lin R-Z, Qi H, Yang Y, Bae H, Melero-Martin JM, Khademhosseini A (2012) Functional human vascular network generated in photocrosslinkable gelatin methacrylate hydrogels. Adv Funct Mater 22:2027–2039. https://doi.org/10.1002/adfm.201101662

Chung JHY, Naficy S, Yue Z, Kapsa R, Quigley A, Moulton SE, Wallace GG (2013) Bio-ink properties and printability for extrusion printing living cells. Biomater Sci 1:763. https://doi.org/10.1039/c3bm00012e

Cohen DL, Lipton JI, Bonassar LJ, Lipson H (2010) Additive manufacturing for in situ repair of osteochondral defects. Biofabrication 2:035004. https://doi.org/10.1088/1758-5082/2/3/035004

Cui X, Breitenkamp K, Finn MG, Lotz M, D'Lima DD (2012) Direct human cartilage repair using three-dimensional bioprinting technology. Tissue Eng Part A 18:1304–1312. https://doi.org/10.1089/ten.TEA.2011.0543

Das S, Pati F, Choi YJ, Rijal G, Shim JH, Kim SW, Ray AR, Cho DW, Ghosh S (2015) Bioprintable, cell-laden silk fibroin-gelatin hydrogel supporting multilineage differentiation of stem cells for fabrication of three-dimensional tissue constructs. Acta Biomater 11:233–246. https://doi.org/10.1016/j.actbio.2014.09.023

Davey SK, Aung A, Agrawal G, Lim HL, Kar M, Varghese S (2015) Embedded 3D photopatterning of hydrogels with diverse and complex architectures for tissue engineering and disease models. Tissue Eng Part C Methods 21:1188–1196. https://doi.org/10.1089/ten.TEC.2015.0179

Dhariwala B, Hunt E, Boland T (2004) Rapid prototyping of tissue-engineering constructs, using photopolymerizable hydrogels and stereolithography. Tissue Eng 10:1316–1322. https://doi.org/10.1089/ten.2004.10.1316

Duan B, Hockaday LA, Kang KH, Butcher JT (2013) 3D Bioprinting of heterogeneous aortic valve conduits with alginate/gelatin hydrogels. J Biomed Mater Res A 101 A:1255–1264. https://doi.org/10.1002/jbm.a.34420

Duan B, Kapetanovic E, Hockaday LA, Butcher JT (2014) Three-dimensional printed trileaflet valve conduits using biological hydrogels and human valve interstitial cells. Acta Biomater 10:1836–1846. https://doi.org/10.1016/j.actbio.2013.12.005

Elomaa L, Teixeira S, Hakala R, Korhonen H, Grijpma DW, Seppälä JV (2011) Preparation of poly (ε-caprolactone)-based tissue engineering scaffolds by stereolithography. Acta Biomater 7:3850–3856. https://doi.org/10.1016/j.actbio.2011.06.039

Elomaa L, Pan C-C, Shanjani Y, Malkovskiy A, Seppälä JV, Yang Y (2015) Three-dimensional fabrication of cell-laden biodegradable poly(ethylene glycol-co-depsipeptide) hydrogels by visible light stereolithography. J Mater Chem B 3:8348–8358. https://doi.org/10.1039/C5TB01468A

Faulkner-Jones A, Fyfe C, Cornelissen D-J, Gardner J, King J, Courtney A, Shu W (2015) Bioprinting of human pluripotent stem cells and their directed differentiation into hepatocyte-like cells for the generation of mini-livers in 3D. Biofabrication 7:044102. https://doi.org/10.1088/1758-5090/7/4/044102

Fedorovich NE, De Wijn JR, Verbout AJ, Alblas J, Dhert WJA (2008) Three-dimensional fiber deposition of cell-laden, viable, patterned constructs for bone tissue printing. Tissue Eng Part A 14:127–133. https://doi.org/10.1089/ten.a.2007.0158

Fedorovich NE, Wijnberg HM, Dhert WJ, Alblas J (2011) Distinct tissue formation by heterogeneous printing of osteo – and endothelial progenitor cells. Tissue Eng Part A 17:2113–2121. https://doi.org/10.1089/ten.tea.2011.0019

Fedorovich NE, Schuurman W, Wijnberg HM, Prins H-J, van Weeren PR, Malda J, Alblas J, Dhert WJA (2012) Biofabrication of osteochondral tissue equivalents by printing topologically defined, cell-laden hydrogel scaffolds. Tissue Eng Part C Methods 18:33–44. https://doi.org/10.1089/ten.TEC.2011.0060

Ferlin KM, Prendergast ME, Miller ML, Kaplan DS, Fisher JP (2016) Influence of 3D printed porous architecture on mesenchymal stem cell enrichment and differentiation. Acta Biomater 32:161–169. https://doi.org/10.1016/j.actbio.2016.01.007

Ferris CJ, Gilmore KG, Wallace GG, In Het Panhuis M (2013a) Biofabrication: an overview of the approaches used for printing of living cells. Appl Microbiol Biotechnol 97:4243–4258

Ferris CJ, Gilmore KJ, Beirne S, McCallum D, Wallace GG, in het Panhuis M (2013b) Bio-ink for on-demand printing of living cells. Biomater Sci 1:224. https://doi.org/10.1039/c2bm00114d

Florián-Algarín V, Acevedo-Rullán A, Co A, Leal GL, Colby RH, Giacomin AJ (2008) Rheology and gelation temperature of aqueous gelatin and sodium alginate solutions. In: AIP Conference Proceedings. AIP, pp 618–620

Gaetani R, Feyen DAM, Verhage V, Slaats R, Messina E, Christman KL, Giacomello A, Doevendans PAFM, Sluijter JPG (2015) Epicardial application of cardiac progenitor cells in a 3D-printed gelatin/hyaluronic acid patch preserves cardiac function after myocardial infarction. Biomaterials 61:339–348. https://doi.org/10.1016/j.biomaterials.2015.05.005

Galante R, Paradiso P, Moutinho MG, Fernandes AI, Mata JLG, Matos APA, Colaço R, Saramago B, Serro AP (2015) About the effect of eye blinking on drug release from pHEMA-based hydrogels: an in vitro study. J Biomater Sci Polym Ed 26:235–251. https://doi.org/10.1080/09205063.2014.994948

Gao G, Schilling AF, Hubbell K, Yonezawa T, Truong D, Hong Y, Dai G, Cui X (2015a) Improved properties of bone and cartilage tissue from 3D inkjet-bioprinted human mesenchymal stem cells by simultaneous deposition and photocrosslinking in PEG-GelMA. Biotechnol Lett 37:2349–2355. https://doi.org/10.1007/s10529-015-1921-2

Gao G, Yonezawa T, Hubbell K, Dai G, Cui X (2015b) Inkjet-bioprinted acrylated peptides and PEG hydrogel with human mesenchymal stem cells promote robust bone and cartilage formation with minimal printhead clogging. Biotechnol J 10:1568–1577. https://doi.org/10.1002/biot.201400635

García-Millán E, Koprivnik S, Otero-Espinar FJ (2015) Drug loading optimization and extended drug delivery of corticoids from pHEMA based soft contact lenses hydrogels via chemical and microstructural modifications. Int J Pharm 487:260–269. https://doi.org/10.1016/j.ijpharm.2015.04.037

Hanson Shepherd JN, Parker ST, Shepherd RF, Gillette MU, Lewis JA, Nuzzo RG (2011) 3D microperiodic hydrogel scaffolds for robust neuronal cultures. Adv Funct Mater 21:47–54. https://doi.org/10.1002/adfm.201001746

He P, Liu Y, Qiao R (2014) Fluid dynamics of the droplet impact processes in cell printing. Microfluid Nanofluidics 18:569–585. https://doi.org/10.1007/s10404-014-1470-3

Highley CB, Rodell CB, Burdick JA (2015) Direct 3D printing of shear-thinning hydrogels into self-healing hydrogels. Adv Mater 27:5075–5079. https://doi.org/10.1002/adma.201501234

Hinton TJ, Jallerat Q, Palchesko RN, Park JH, Grodzicki MS, Shue H-J, Ramadan MH, Hudson AR, Feinberg AW (2015) Three-dimensional printing of complex biological structures by freeform reversible embedding of suspended hydrogels. Sci Adv 1:1–10. https://doi.org/10.1126/sciadv.1500758

Hoare TR, Kohane DS (2008) Hydrogels in drug delivery: progress and challenges. Polymer (Guildf) 49:1993–2007. https://doi.org/10.1016/j.polymer.2008.01.027

Hockaday LA, Kang KH, Colangelo NW, Cheung PYC, Duan B, Malone E, Wu J, Girardi LN, Bonassar LJ, Lipson H, Chu CC, Butcher JT (2012) Rapid 3D printing of anatomically accurate and mechanically heterogeneous aortic valve hydrogel scaffolds. Biofabrication 4:035005. https://doi.org/10.1088/1758-5082/4/3/035005

Hong S, Sycks D, Chan HF, Lin S, Lopez GP, Guilak F, Leong KW, Zhao X (2015) 3D printing of highly stretchable and tough hydrogels into complex, cellularized structures. Adv Mater 27:4035–4040. https://doi.org/10.1002/adma.201501099

Hsieh F-Y, Lin H-H, Hsu S-H (2015) 3D bioprinting of neural stem cell-laden thermoresponsive biodegradable polyurethane hydrogel and potential in central nervous system repair. Biomaterials 71:48–57. https://doi.org/10.1016/j.biomaterials.2015.08.028

Hu J, Hou Y, Park H, Choi B, Hou S, Chung A, Lee M (2012) Visible light crosslinkable chitosan hydrogels for tissue engineering. Acta Biomater 8:1730–1738. https://doi.org/10.1016/j.actbio.2012.01.029

Hynes RO (2002) Integrins: bidirectional, allosteric signaling machines. Cell 110:673–687. https://doi.org/10.1016/S0092-8674(02)00971-6

Ifkovits JL, Burdick JA (2007) Review: photopolymerizable and degradable biomaterials for tissue engineering applications. Tissue Eng 13:2369–2385. https://doi.org/10.1089/ten.2007.0093

Jung JW, Lee J-S, Cho D-W (2016) Computer-aided multiple-head 3D printing system for printing of heterogeneous organ/tissue constructs. Sci Rep 6:21685. https://doi.org/10.1038/srep21685

Kesti M, Müller M, Becher J, Schnabelrauch M, D'Este M, Eglin D, Zenobi-Wong M (2015) A versatile bioink for three-dimensional printing of cellular scaffolds based on thermally and photo-triggered tandem gelation. Acta Biomater 11:162–172. https://doi.org/10.1016/j.actbio.2014.09.033

Khalil S, Sun W (2007) Biopolymer deposition for freeform fabrication of hydrogel tissue constructs. Mater Sci Eng C 27:469–478. https://doi.org/10.1016/j.msec.2006.05.023

Koch L, Deiwick A, Schlie S, Michael S, Gruene M, Coger V, Zychlinski D, Schambach A, Reimers K, Vogt PM, Chichkov B (2012) Skin tissue generation by laser cell printing. Biotechnol Bioeng 109:1855–1863. https://doi.org/10.1002/bit.24455

Kolesky DB, Truby RL, Gladman AS, Busbee TA, Homan KA, Lewis JA (2014) 3D bioprinting of vascularized, heterogeneous cell-laden tissue constructs. Adv Mater 26:3124–3130. https://doi.org/10.1002/adma.201305506

Kundu J, Shim J-H, Jang J, Kim S-W, Cho D-W (2015) An additive manufacturing-based PCL-alginate-chondrocyte bioprinted scaffold for cartilage tissue engineering. J Tissue Eng Regen Med 9:1286–1297. https://doi.org/10.1002/term.1682

Lee W, Debasitis JC, Lee VK, Lee J-H, Fischer K, Edminster K, Park J-K, Yoo S-S (2009) Multi-layered culture of human skin fibroblasts and keratinocytes through three-dimensional freeform fabrication. Biomaterials 30:1587–1595. https://doi.org/10.1016/j.biomaterials.2008.12.009

Lee Y-B, Polio S, Lee W, Dai G, Menon L, Carroll RS, Yoo S-S (2010) Bio-printing of collagen and VEGF-releasing fibrin gel scaffolds for neural stem cell culture. Exp Neurol 223:645–652. https://doi.org/10.1016/j.expneurol.2010.02.014

Lee H, Ahn S, Bonassar LJ, Kim G (2013) Cell(MC3T3-E1)-printed poly(ϵ-caprolactone)/alginate hybrid scaffolds for tissue regeneration. Macromol Rapid Commun 34:142–149. https://doi.org/10.1002/marc.201200524

Lee VK, Lanzi AM, Ngo H, Yoo SS, Vincent PA, Dai G (2014) Generation of multi-scale vascular network system within 3D hydrogel using 3D bio-printing technology. Cell Mol Bioeng 7:460–472. https://doi.org/10.1007/s12195-014-0340-0

Lee JW, Choi YJ, Yong WJ, Pati F, Shim JH, Kang KS, Kang IH, Park J, Cho DW (2016) Development of a 3D cell printed construct considering angiogenesis for liver tissue engineering. Biofabrication 8:15007. https://doi.org/10.1088/1758-5090/8/1/015007

Levato R, Visser J, Planell JA, Engel E, Malda J, Mateos-Timoneda MA (2014) Biofabrication of tissue constructs by 3D bioprinting of cell-laden microcarriers. Biofabrication 6:035020. https://doi.org/10.1088/1758-5082/6/3/035020

Li B, Wang L, Xu F, Gang X, Demirci U, Wei D, Li Y, Feng Y, Jia D, Zhou Y (2015) Hydrosoluble, UV-crosslinkable and injectable chitosan for patterned cell-laden microgel and rapid transdermal curing hydrogel in vivo. Acta Biomater 22:59–69. https://doi.org/10.1016/j.actbio.2015.04.026

Lin H, Zhang D, Alexander PG, Yang G, Tan J, Cheng AW-M, Tuan RS (2013) Application of visible light-based projection stereolithography for live cell-scaffold fabrication with designed architecture. Biomaterials 34:331–339. https://doi.org/10.1016/j.biomaterials.2012.09.048

Ma Y, Ji Y, Huang G, Ling K, Zhang X, Xu F (2015) Bioprinting 3D cell-laden hydrogel microarray for screening human periodontal ligament stem cell response to extracellular matrix. Biofabrication 7:044105. https://doi.org/10.1088/1758-5090/7/4/044105

Mapili G, Lu Y, Chen S, Roy K (2005) Laser-layered microfabrication of spatially patterned functionalized tissue-engineering scaffolds. J Biomed Mater Res B Appl Biomater 75:414–424. https://doi.org/10.1002/jbm.b.30325

Markstedt K, Mantas A, Tournier I, Martínez Ávila H, Hägg D, Gatenholm P (2015) 3D bioprinting human chondrocytes with nanocellulose-alginate bioink for cartilage tissue engineering applications. Biomacromolecules 16:1489–1496. https://doi.org/10.1021/acs.biomac.5b00188

Melchels FPW, Feijen J, Grijpma DW (2009) A poly(D,L-lactide) resin for the preparation of tissue engineering scaffolds by stereolithography. Biomaterials 30:3801–3809. https://doi.org/10.1016/j.biomaterials.2009.03.055

Melchels FPW, Feijen J, Grijpma DW (2010) A review on stereolithography and its applications in biomedical engineering. Biomaterials 31:6121–6130. https://doi.org/10.1016/j.biomaterials.2010.04.050

Melchels FPW, Dhert WJA, Hutmacher DW, Malda J (2014) Development and characterisation of a new bioink for additive tissue manufacturing. J Mater Chem B 2:2282. https://doi.org/10.1039/c3tb21280g

Mironi-Harpaz I, Wang DY, Venkatraman S, Seliktar D (2012) Photopolymerization of cell-encapsulating hydrogels: crosslinking efficiency versus cytotoxicity. Acta Biomater 8:1838–1848. https://doi.org/10.1016/j.actbio.2011.12.034

Mohanty S, Alm M, Hemmingsen M, Dolatshahi-Pirouz A, Trifol J, Thomsen P, Dufva M, Wolff A, Emnéus J (2016) 3D printed silicone-hydrogel scaffold with enhanced physicochemical properties. Biomacromolecules 17:1321. https://doi.org/10.1021/acs.biomac.5b01722

Moraes C, Simon AB, Putnam AJ, Takayama S (2013) Aqueous two-phase printing of cell-containing contractile collagen microgels. Biomaterials 34:9623–9631. https://doi.org/10.1016/j.biomaterials.2013.08.046

Müller M, Becher J, Schnabelrauch M, Zenobi-Wong M (2015) Nanostructured pluronic hydrogels as bioinks for 3D bioprinting. Biofabrication 7:035006. https://doi.org/10.1088/1758-5090/7/3/035006

Murphy SV, Atala A (2014) 3D bioprinting of tissues and organs. Nat Biotechnol 32:773–785. https://doi.org/10.1038/nbt.2958

Nair K, Gandhi M, Khalil S, Yan KC, Marcolongo M, Barbee K, Sun W (2009) Characterization of cell viability during bioprinting processes. Biotechnol J 4:1168–1177. https://doi.org/10.1002/biot.200900004

Nakamura M, Kobayashi A, Takagi F, Watanabe A, Hiruma Y, Ohuchi K, Iwasaki Y, Horie M, Morita I, Takatani S (2005) Biocompatible inkjet printing technique for designed seeding of individual living cells. Tissue Eng 11:1658–1666. https://doi.org/10.1089/ten.2005.11.1658

Ouyang L, Yao R, Chen X, Na J, Sun W (2015a) 3D printing of HEK 293FT cell-laden hydrogel into macroporous constructs with high cell viability and normal biological functions. Biofabrication 7:015010. https://doi.org/10.1088/1758-5090/7/1/015010

Ouyang L, Yao R, Mao S, Chen X, Na J, Sun W (2015b) Three-dimensional bioprinting of embryonic stem cells directs highly uniform embryoid body formation. Biofabrication 7:044101. https://doi.org/10.1088/1758-5090/7/4/044101

Ovsianikov A, Gruene M, Pflaum M, Koch L, Maiorana F, Wilhelmi M, Haverich A, Chichkov B (2010) Laser printing of cells into 3D scaffolds. Biofabrication 2:014104. https://doi.org/10.1088/1758-5082/2/1/014104

Park JY, Shim J-H, Choi S-A, Jang J, Kim M, Lee SH, Cho D-W (2015) 3D printing technology to control BMP-2 and VEGF delivery spatially and temporally to promote large-volume bone regeneration. J Mater Chem B 3:5415–5425. https://doi.org/10.1039/C5TB00637F

Pataky K, Braschler T, Negro A, Renaud P, Lutolf MP, Brugger J (2012) Microdrop printing of hydrogel bioinks into 3D tissue-like geometries. Adv Mater 24:391–396. https://doi.org/10.1002/adma.201102800

Pati F, Jang J, Ha D-H, Won Kim S, Rhie J-W, Shim J-H, Kim D-H, Cho D-W (2014) Printing three-dimensional tissue analogues with decellularized extracellular matrix bioink. Nat Commun 5:3935. https://doi.org/10.1038/ncomms4935

Pati F, Ha D-H, Jang J, Han HH, Rhie JW, Cho DW (2015) Biomimetic 3D tissue printing for soft tissue regeneration. Biomaterials 62:164–175. https://doi.org/10.1016/j.biomaterials.2015.05.043

Pereira RF, Bártolo PJ (2015) 3D bioprinting of photocrosslinkable hydrogel constructs. J Appl Polym Sci 132. https://doi.org/10.1002/app.42458

Petit V, Thiery J-P (2000) Focal adhesions: structure and dynamics. Biol Cell 92:477–494. https://doi.org/10.1016/S0248-4900(00)01101-1

Pietrucha K (2005) Changes in denaturation and rheological properties of collagen-hyaluronic acid scaffolds as a result of temperature dependencies. Int J Biol Macromol 36:299–304. https://doi.org/10.1016/j.ijbiomac.2005.07.004

Qiu Y, Park K (2001) Environment-sensitive hydrogels for drug delivery. Adv Drug Deliv Rev 53:321–339. https://doi.org/10.1016/S0169-409X(01)00203-4

Rezende RA, Bártolo PJ, Mendes A, Filho RM (2009) Rheological behavior of alginate solutions for biomanufacturing. J Appl Polym Sci 113:3866–3871. https://doi.org/10.1002/app.30170

Ringeisen BR, Kim H, Barron JA, Krizman DB, Chrisey DB, Jackman S, Auyeung RYC, Spargo BJ (2004) Laser printing of pluripotent embryonal carcinoma cells. Tissue Eng 10:483–491. https://doi.org/10.1089/107632704323061843

Roth EA, Xu T, Das M, Gregory C, Hickman JJ, Boland T (2004) Inkjet printing for high-throughput cell patterning. Biomaterials 25:3707–3715. https://doi.org/10.1016/j.biomaterials.2003.10.052

Rouillard AD, Berglund CM, Lee JY, Polacheck WJ, Tsui Y, Bonassar LJ, Kirby BJ (2011) Methods for photocrosslinking alginate hydrogel scaffolds with high cell viability. Tissue Eng Part C Methods 17:173–179. https://doi.org/10.1089/ten.TEC.2009.0582

Rutz AL, Hyland KE, Jakus AE, Burghardt WR, Shah RN (2015) A multimaterial bioink method for 3D printing tunable, cell-compatible hydrogels. Adv Mater 27:1607–1614. https://doi.org/10.1002/adma.201405076

Schmedlen RH, Masters KS, West JL (2002) Photocrosslinkable polyvinyl alcohol hydrogels that can be modified with cell adhesion peptides for use in tissue engineering. Biomaterials 23:4325–4332. https://doi.org/10.1016/S0142-9612(02)00177-1

Schuurman W, Khristov V, Pot MW, van Weeren PR, Dhert WJA, Malda J (2011) Bioprinting of hybrid tissue constructs with tailorable mechanical properties. Biofabrication 3:021001. https://doi.org/10.1088/1758-5082/3/2/021001

Schuurman W, Levett PA, Pot MW, van Weeren PR, Dhert WJA, Hutmacher DW, Melchels FPW, Klein TJ, Malda J (2013) Gelatin-methacrylamide hydrogels as potential biomaterials for fabrication of tissue-engineered cartilage constructs. Macromol Biosci 13:551–561. https://doi.org/10.1002/mabi.201200471

Sher P, Oliveira SM, Borges J, Mano JF (2015) Assembly of cell-laden hydrogel fiber into non-liquefied and liquefied 3D spiral constructs by perfusion-based layer-by-layer technique. Biofabrication 7:011001. https://doi.org/10.1088/1758-5090/7/1/011001

Shim J-H, Lee J-S, Kim JY, Cho D-W (2012) Bioprinting of a mechanically enhanced three-dimensional dual cell-laden construct for osteochondral tissue engineering using a multi-head tissue/organ building system. J Micromech Microeng 22:085014. https://doi.org/10.1088/0960-1317/22/8/085014

Skardal A, Atala A (2015) Biomaterials for integration with 3-D bioprinting. Ann Biomed Eng 43:730–746. https://doi.org/10.1007/s10439-014-1207-1

Skardal A, Zhang J, McCoard L, Xu X, Oottamasathien S, Prestwich GD (2010) Photocrosslinkable hyaluronan-gelatin hydrogels for two-step bioprinting. Tissue Eng Part A 16:2675–2685. https://doi.org/10.1089/ten.TEA.2009.0798

Smith CM, Stone AL, Parkhill RL, Stewart RL, Simpkins MW, Kachurin AM, Warren WL, Williams SK (2004) Three-dimensional bioassembly tool for generating viable tissue-engineered constructs. Tissue Eng 10:1566–1576. https://doi.org/10.1089/ten.2004.10.1566

Smith CM, Christian JJ, Warren WL, Williams SK (2007) Characterizing environmental factors that impact the viability of tissue-engineered constructs fabricated by a direct-write bioassembly tool. Tissue Eng 13:373–383. https://doi.org/10.1089/ten.2006.0101

Song SJ, Choi J, Park YD, Hong S, Lee JJ, Ahn CB, Choi H, Sun K (2011) Sodium alginate hydrogel-based bioprinting using a novel multinozzle bioprinting system. Artif Organs 35:1132–1136. https://doi.org/10.1111/j.1525-1594.2011.01377.x

Tabriz AG, Hermida MA, Leslie NR, Shu W (2015) Three-dimensional bioprinting of complex cell laden alginate hydrogel structures. Biofabrication 7:045012. https://doi.org/10.1088/1758-5090/7/4/045012

Takada Y, Ye X, Simon S (2007) The integrins. Genome Biol 8(215). https://doi.org/10.1186/gb-2007-8-5-215

Tsai YC, Li S, SG H, Chang WC, Jeng US, Hsu SH (2015) Synthesis of thermoresponsive amphiphilic polyurethane gel as a new cell printing material near body temperature. ACS Appl Mater Interfaces 7:27613–27623. https://doi.org/10.1021/acsami.5b10697

Visser J, Peters B, Burger TJ, Boomstra J, Dhert WJA, Melchels FPW, Malda J (2013) Biofabrication of multi-material anatomically shaped tissue constructs. Biofabrication 5:035007. https://doi.org/10.1088/1758-5082/5/3/035007

Wallace J, Wang MO, Thompson P, Busso M, Belle V, Mammoser N, Kim K, Fisher JP, Siblani A, Xu Y, Welter JF, Lennon DP, Sun J, Caplan AI, Dean D (2014) Validating continuous digital

light processing (cDLP) additive manufacturing accuracy and tissue engineering utility of a dye-initiator package. Biofabrication 6:015003. https://doi.org/10.1088/1758-5082/6/1/015003
Wang W, Huang Y, Grujicic M, Chrisey DB (2008) Study of impact-induced mechanical effects in cell direct writing using smooth particle hydrodynamic method. J Manuf Sci Eng 130:021012. https://doi.org/10.1115/1.2896118
Wang MO, Piard CM, Melchiorri A, Dreher ML, Fisher JP (2015a) Evaluating changes in structure and cytotoxicity during in vitro degradation of three-dimensional printed scaffolds. Tissue Eng Part A 21:1642–1653. https://doi.org/10.1089/ten.TEA.2014.0495
Wang Z, Zhang Y, Zhu J, Dong S, Jiang T, Zhou Y, Zhang X (2015b) In vitro investigation of a tissue-engineered cell-tendon complex mimicking the transitional architecture at the ligament-bone interface. J Biomater Appl 29:1180–1192. https://doi.org/10.1177/0885328214555168
Wei J, Wang J, Su S, Wang S, Qiu J, Zhang Z, Christopher G, Ning F, Cong W (2015) 3D printing of an extremely tough hydrogel. RSC Adv 5:81324–81329. https://doi.org/10.1039/C5RA16362E
Williams CG, Malik AN, Kim TK, Manson PN, Elisseeff JH (2005) Variable cytocompatibility of six cell lines with photoinitiators used for polymerizing hydrogels and cell encapsulation. Biomaterials 26:1211–1218. https://doi.org/10.1016/j.biomaterials.2004.04.024
Xu Y, Wang X (2015) Fluid and cell behaviors along a 3D printed alginate/gelatin/fibrin channel. Biotechnol Bioeng 112:1683–1695. https://doi.org/10.1002/bit.25579
Xu T, Jin J, Gregory C, Hickman JJJJ, Boland T (2005) Inkjet printing of viable mammalian cells. Biomaterials 26:93–99. https://doi.org/10.1016/j.biomaterials.2004.04.011
Xu T, Zhao W, Atala A, Yoo JJ, Forest W, Salem W (2006) Bio-printing of living organized tissues using an inkjet technology. FASEB J 21:131–134
Xu M, Wang X, Yan Y, Yao R, Ge Y (2010) An cell-assembly derived physiological 3D model of the metabolic syndrome, based on adipose-derived stromal cells and a gelatin/alginate/fibrinogen matrix. Biomaterials 31:3868–3877. https://doi.org/10.1016/j.biomaterials.2010.01.111
Xu T, Zhao W, Zhu JM, Albanna MZ, Yoo JJ, Atala A (2013a) Complex heterogeneous tissue constructs containing multiple cell types prepared by inkjet printing technology. Biomaterials 34:130–139. https://doi.org/10.1016/j.biomaterials.2012.09.035
Xu T, Binder KW, Albanna MZ, Dice D, Zhao W, Yoo JJ, Atala A (2013b) Hybrid printing of mechanically and biologically improved constructs for cartilage tissue engineering applications. Biofabrication 5:015001. https://doi.org/10.1088/1758-5082/5/1/015001
Yan Y, Wang X, Pan Y, Liu H, Cheng J, Xiong Z, Lin F, Wu R, Zhang R, Lu Q (2005) Fabrication of viable tissue-engineered constructs with 3D cell-assembly technique. Biomaterials 26:5864–5871. https://doi.org/10.1016/j.biomaterials.2005.02.027
Yu Y, Zhang Y, Martin JA, Ozbolat IT (2013) Evaluation of cell viability and functionality in vessel-like bioprintable cell-laden tubular channels. J Biomech Eng 135:91011. https://doi.org/10.1115/1.4024575
Zhang Y, Yu Y, Chen H, Ozbolat IT (2013) Characterization of printable cellular micro-fluidic channels for tissue engineering. Biofabrication 5:025004. https://doi.org/10.1088/1758-5082/5/2/025004
Zhang M, Vora A, Han W, Wojtecki RJ, Maune H, Le ABA, Thompson LE, McClelland GM, Ribet F, Engler AC, Nelson A (2015) Dual-responsive hydrogels for direct-write 3D printing. Macromolecules 48:6482–6488. https://doi.org/10.1021/acs.macromol.5b01550
Zhao Y, Yao R, Ouyang L, Ding H, Zhang T, Zhang K, Cheng S, Sun W (2014) Three-dimensional printing of Hela cells for cervical tumor model in vitro. Biofabrication 6:035001. https://doi.org/10.1088/1758-5082/6/3/035001
Zhao Y, Li Y, Mao S, Sun W, Yao R (2015) The influence of printing parameters on cell survival rate and printability in microextrusion-based 3D cell printing technology. Biofabrication 7:045002. https://doi.org/10.1088/1758-5090/7/4/045002